



Published in final edited form as:

*J Immunol.* 2016 August 15; 197(4): 1308–1321. doi:10.4049/jimmunol.1502481.

## IL-10 regulates memory T cell development and the balance between Th1 and Tfh responses during an acute viral infection

Yuan Tian<sup>\*</sup>, Sarah B. Mollo<sup>†,‡</sup>, Laurie E. Harrington<sup>†</sup>, and Allan J. Zajac<sup>\*</sup>

<sup>\*</sup>Department of Microbiology, University of Alabama at Birmingham, Birmingham, AL 35294, United States

<sup>†</sup>Department of Cell, Developmental and Integrative Biology, University of Alabama at Birmingham, Birmingham, AL 35294, United States

### Abstract

T cells provide protective immunity against infections by differentiating into effector cells that contribute to rapid pathogen control and by forming memory populations that survive over time and confer long-term protection. Thus, understanding the factors that regulate the development of effective T cell responses is beneficial for the design of vaccines and immune based therapies against infectious diseases. Cytokines play important roles in shaping T cell responses, and IL-10 has been shown to modulate the differentiation of CD4 and CD8 T cells. In this study, we report that IL-10 functions in a cell-extrinsic manner early following acute lymphocytic choriomeningitis virus (LCMV) infection to suppress the magnitude of effector T helper type 1 (Th1) responses as well as the generation of memory CD4 and CD8 T cells. We further demonstrate that the blockade of IL-10 signaling during the priming phase refines the functional quality of memory CD4 and CD8 T cells. This inhibition strategy resulted in a lower frequency of virus-specific follicular helper T cells (Tfh) and increased the Th1 to Tfh ratio. Nevertheless, neither germinal center B cells nor LCMV-specific antibody levels were influenced by the blockade. Thus, our studies show that IL-10 influences the balance between Th1 and Tfh cell differentiation and negatively regulates the development of functionally mature memory T cells.

### Introduction

T cell responses are initiated and shaped by antigenic signals, costimulatory molecules, and cytokines. IL-10 is a general suppressive cytokine that plays important roles in regulating immune responses against infections (1, 2). IL-10 can act both directly and indirectly on CD4 and CD8 T cells to inhibit their expansion, function, and memory formation (3–10). IL-10-mediated inhibitory signals contribute to T cell exhaustion during chronic viral infections, and the loss of IL-10 or IL-10 signaling restores the anti-viral T cell response and promotes viral clearance (3–6). Notably, the blockade of IL-10 receptor alone or with the blockade of programmed death-ligand 1 (PD-L1) improves anti-viral T cell responses and accelerates the clearance of chronic lymphocytic choriomeningitis virus (LCMV) infection,

Address correspondence to: Dr. Allan J. Zajac, University of Alabama at Birmingham, Department of Microbiology, 845 19th Street South, BBRB 446; Box 23, Birmingham, AL 35294-2170. Tel: (205) 975-5644, Fax: (205) 975-5482, azajac@uab.edu.

<sup>‡</sup>Present address: Food and Drug Administration, Silver Spring, MD 20993

highlighting the therapeutic potential of neutralizing IL-10 activity (3, 4, 11, 12). Furthermore, IL-10, together with IL-4 and TGF $\beta$ , dampens the production of IFN $\gamma$  by antigen-experienced CD8 T cells in response to cytokine stimulation (13).

Despite its immunosuppressive functions during chronic infections, the roles of IL-10 in shaping CD8 T cell responses following acute infections are more complex. While a previous study suggests that IL-10 plays a minimal role in the differentiation of memory CD8 T cells following acute LCMV infection (7), more recent studies indicate that IL-10 promotes the maturation of memory CD8 T cells (14, 15). Additionally, both positive and negative effects of IL-10 on the generation of effector and memory CD8 T cells have been reported following *Listeria monocytogenes* infection (8, 16). Furthermore, it has been suggested that IL-10 may have opposing effects on primary and secondary CD8 T cell responses in response to peptide simulation *in vitro* (17). Therefore, the actions of IL-10 on CD8 T cells may be influenced by additional signals such as antigenic and inflammatory signals, and it is crucial to define such signals in order to better understand how IL-10 regulates anti-viral CD8 T cell responses. In addition to T cell responses, antibodies also provide protective immunity against invading pathogens. Germinal centers (GCs) are essential for the production of high-affinity antibodies and their development relies on follicular helper T (Tfh) cells (18). In contrast to Tfh cells, follicular regulatory T (Tfr) cells exert immunosuppressive effects on GC responses (19–21). Although much has been learned about the actions of IL-10 on anti-viral type 1 helper T (Th1) cells and CD8 T cells, whether IL-10 modulates the differentiation of Tfh and Tfr cells as well as the formation of GC responses after viral infections is less well defined.

In this study we set out to decipher whether IL-10 regulates the differentiation of memory T cells, CD4 T cell subsets, and GC B cells following acute LCMV infection. We report that IL-10 functions early following infection, in an indirect manner, to restrict the magnitude of effector Th1 CD4 T cells and also negatively impacts the formation and function of memory Th1 responses. Although the blockade of IL-10 signaling during the priming phase does not influence the anti-viral antibody response, we observed a decreased frequency of virus-specific Tfh cells as well as an elevated ratio of Th1 to Tfh cells in treated mice; however, the absolute number of virus-specific Tfh cells was unaffected. Surprisingly, we discovered that IL-10 suppresses the development and functional maturation of memory CD8 T cells. By analyzing two epitope-specific CD8 T cell populations, we found that the effect of IL-10 was more pronounced on LCMV NP396-specific CD8 T cells than their GP33-specific counterparts, which supports the hypothesis that the actions of IL-10-induced signals on CD8 T cells may be influenced by the degree of antigenic stimulation. Collectively, our data demonstrate that IL-10 acts indirectly to restrict the maturation of memory CD4 and CD8 T cells and modulates the balance between Th1 and Tfh cell differentiation.

## Materials and Methods

### Mice

C57BL/6J (WT), B6.129P2-*Il10<sup>tm1Cgn</sup>*/J (IL-10<sup>-/-</sup>), B6.SJL-*Ptprca<sup>a</sup>Pepcb<sup>b</sup>*/BoyJ (CD45.1), B6.129S2-*Il10rb<sup>tm1Agt</sup>*/J (IL-10R<sup>-/-</sup>), and B6.129S7-*Rag1<sup>tm1Mom</sup>*/J (RAG-1<sup>-/-</sup>) were purchased from The Jackson Laboratory (Bar Harbor, ME). The IFN $\gamma$ /Thy1.1 Knock-in

mice have been previously described (22). IL-10<sup>-/-</sup> IFN $\gamma$ /Thy1.1 Knock-in mice were generated by crossing the IL-10<sup>-/-</sup> mice with IFN $\gamma$ /Thy1.1 Knock-in mice. Mice that were homozygous for the IFN $\gamma$ /Thy1.1 allele were used in these studies. Thy1.1 SMARTA TCR transgenic mice were kindly provided by Dr. Dorian McGavern (Scripps Research Institute, CA) with permission from Dr. Annette Oxenius (ETH Zurich). All mice were bred and maintained in fully accredited facilities at the University of Alabama at Birmingham.

### Infections and cell transfers

Acute infections were established by i.p injection with 2 $\times$ 10<sup>5</sup> pfu LCMV-Armstrong (LCMV). Viral titers of serum and spleen samples were determined by plaque assays using Vero cell monolayers (23). For cell transfers, CD4 T cells were purified from the spleens of Thy1.1 SMARTA TCR transgenic mice using the Dynabeads FlowComp Mouse CD4 Purification Kit (Invitrogen) according to the manufacturer's directions, and 10<sup>5</sup> cells were transferred by i.p. injection into recipient mice.

### *In vivo* anti-IL-10R blockade

Monoclonal antibodies against IL-10 receptor (clone: 1B1.3A; Bio X Cell) were administered at a dose of 250  $\mu$ g/mouse by i.p. injection on days 0, 2, 4, and 6 following LCMV infection.

### Generation of mixed bone marrow chimeras

Bone marrow chimeras were generated essentially as previously described (24). Briefly, suspensions of bone marrow, obtained from the tibias and femurs of CD45.1 IL-10R<sup>+/+</sup> and CD45.2 IL-10R<sup>-/-</sup> mice were depleted of T cells using anti-CD5 (Ly-1) microbeads (Miltenyi Biotec; Auburn, CA). RAG-1<sup>-/-</sup> recipient mice were exposed to two doses of radiation (~500 rads each) from a <sup>137</sup>Cs source, given 3–4 hours apart. These irradiated recipients were then reconstituted by i.v. injection of 5 $\times$ 10<sup>6</sup> CD45.1 IL-10R<sup>+/+</sup> T cell depleted bone marrow cells and an equal number of CD45.2 IL-10R<sup>-/-</sup> cells. Mice were provided chlorinated acidified water containing neomycin for 6 weeks following reconstitution.

### Flow cytometry

Single cell suspensions of splenocytes were stained with various combinations of the following antibodies (all purchased from eBioscience unless indicated otherwise): anti-B cell lymphoma 6 (Bcl6) Brilliant Violet 421 (K112-91; BD Biosciences), anti-CD3 PerCP-Cy5.5 (17A2; BioLegend), anti-CD4 FITC, PerCP-Cy5.5, or PE-Cy7 (RM4-5), anti-CD8 FITC, PerCP-Cy5.5, or Pacific-Blue (53-6.7; BioLegend), anti-CD19 PE-Cy7, allophycocyanin-eFluor780, or Brilliant Violet 510 (1D3, BD Biosciences), anti-CD25 Alexa-Fluor488 (PC61.5), anti-CD44 V500 (IM7; BD Biosciences), anti-CD45.1 allophycocyanin-eFluor780 (A20), anti-CD45.2 FITC or PerCP-Cy5.5 (104; BioLegend), anti-CD95 PE (Jo2, BD Biosciences), anti-CD127 PE (A7R34), anti-eomesodermin (Eomes) PE (Dan11mag), anti-Foxp3 FITC (FJK-16s), anti-IL-2 allophycocyanin (JES6-5H4), anti-IFN $\gamma$  eFluor450 (XMG1.2), anti-KLRG1 PE-Cy7 (2F1), anti-Ly6C PE-Cy7 (HK1.4), anti-PD-1 PE-Cy7 (RMP1-30), anti-PNA FITC (prepared in the lab), anti-PSGL1 Brilliant Violet

421 (2PH1; BD Biosciences), anti-SLAM PE-Cy7 (TC15-12F12.2; BioLegend), anti-T-bet Alexa647 (eBio4B10), anti-Thy1.1 PE (OX-7; BD Biosciences), anti-TNF $\alpha$  FITC (MP6-XT22). MHC class I tetramer staining was performed essentially as previously described (25). For MHC class II tetramer staining, cell suspensions were stained with PE-labeled I-A<sup>b</sup> (GP66-77) tetramer (provided by National Institutes of Health Tetramer Core Facility) at 37°C for 75 min. For CXCR5 staining, cell suspensions were stained with anti-CXCR5-biotin (2G8; BD Biosciences) at 37°C for 45 min, washed and then stained with streptavidin-allophycocyanin (Invitrogen). In order to verify the specificity of the CXCR5-biotin/ streptavidin-allophycocyanin staining, controls were routinely performed in which the primary anti-CXCR5-biotin antibody was omitted. Intracellular staining for Bcl6, Eomes, Foxp3, and T-bet were performed after fixation and permeabilization using the Foxp3/transcription factor staining buffer set (eBioscience). For the analysis of cytokine production splenocytes were stimulated with antigenic peptides and intracellular staining for TNF $\alpha$ , IFN $\gamma$ , and IL-2 performed after fixation and permeabilization using the BD Cytofix/ Cytoperm kit (25). Samples were acquired using an LSR II flow cytometer (BD Biosciences), and data were analyzed using FlowJo software (Tree Star; Ashland, OR).

### Antibody titrations

96-well polystyrene ELISA plates (Nunc) were coated with LCMV clone 13-infected BHK-21 cell lysate overnight at room temperature. After blocking with PBS supplemented with 10% FCS, 0.2% Tween 20, and 0.5 mM thimerosal, three-fold serial dilutions of serum samples were incubated for 90 min at room temperature. Plates were washed with PBS supplemented with 0.5% Tween 20 and incubated with horseradish peroxidase (HRP)-labeled goat anti-mouse IgG $\gamma$ , IgG1, IgG2b, IgG2c, and IgG3 antibodies (SouthernBiotech). After washing, plates were incubated with stabilized hydrogen peroxide and tetramethylbenzidine (Substrate Reagent Pack; R&D systems) according to the manufacturer's instructions, and the reaction was stopped by adding 2N H<sub>2</sub>SO<sub>4</sub>. Optical density (OD) values at 450 nm were determined using a microplate reader (Molecular Devices).

### Statistical analysis

Two-tailed paired Student's t test was used to determine statistical significance between IL-10R<sup>+/+</sup> and IL-10R<sup>-/-</sup> T cell populations in mixed bone marrow chimeras. In other experiments, two-tailed unpaired Student's t test was used to determine statistical significance between groups. *p* values were calculated using Prism software (Graph Pad; La Jolla, CA).

## Results

### IL-10 does not control the differentiation of GC B cells during the priming phase of acute LCMV infection

Previous studies indicate that IL-10 modulates the fate of GC B cells by promoting the differentiation of plasma cells at the expense of memory B cells (26, 27). In addition, IL-10 has been suggested to inhibit GC responses in the context of UV irradiation and lupus (28, 29). However, whether IL-10 regulates the generation of GC B cells during viral infections

is less well defined. To investigate whether IL-10 restricts the development of GCs following viral infection, we infected cohorts of wild-type (WT) mice with LCMV-Armstrong. We treated infected mice with anti-IL-10 receptor ( $\alpha$ IL-10R) antibodies at days 0, 2, 4, and 6 following infection and analyzed B cell and antibody responses during the effector (day 8) and memory (day 30) phases (Fig. 1A). The frequencies and numbers of GC B cells were similar in the treated and untreated cohorts analyzed at days 8 (Fig. 1B, D) and 30 (Fig. 1C, E) post infection. In addition, the titers of LCMV-specific total IgG and IgG subclasses were also similar between treated and untreated mice (Fig. 1F, G and data not shown).

In separate experiments we evaluated viral titers in the serum and spleens of infected control and  $\alpha$ IL-10R treated mice. In both cohorts viremia was generally undetectable ( $<50$  pfu/ml) at all time points checked. Splenic viral titers were similar ( $p=0.1024$ ) in the control ( $8.2\pm 3.7 \times 10^6$  pfu/g) and treated ( $2.3\pm 2.0 \times 10^7$  pfu/g) cohorts at 4 days post infection. By eight days splenic viral levels were below the limits of detection ( $<2.8 \times 10^2$  pfu/g) in 3 of 6 control animals as well as in 4 of 6 of the treated mice. Titers were minimal in the remaining 3 control ( $1.3\pm 0.8 \times 10^3$  pfu/g) and 2 treated ( $3.3\pm 0.3 \times 10^2$  pfu/g) mice, and were undetectable in all mice by the next time point checked, at day 12. Thus, no marked differences in viral levels were detected. Together, these data demonstrate that IL-10 signaling during the priming phase of acute LCMV infection does not influence the generation or maintenance of the GC response, and the tempo of viral control is unchanged by IL-10 receptor blockade.

### IL-10 regulates anti-viral CD4 T cell responses

We next used IFN $\gamma$ /Thy1.1 knock-in reporter mice to evaluate the importance of IL-10 in controlling anti-viral CD4 Th1 responses. In these reporter mice IFN $\gamma$  transcript-positive cells are marked by the expression of Thy1.1, and we have previously shown that the Thy1.1<sup>+</sup> CD4 T cell subset which develops in these mice following acute infection encompasses the LCMV-specific population (22). Comparison of the expression of Thy1.1 by CD4 T cells in WT and IL-10<sup>-/-</sup> IFN $\gamma$ /Thy1.1 reporter mice at 8 days following LCMV infection revealed that a greater fraction and number of Thy1.1<sup>+</sup> CD4 T cells developed in the absence of IL-10 (Fig. 2A, B). In addition, the intensity of Thy1.1 expression by CD4 T cells was higher in IL-10<sup>-/-</sup> IFN $\gamma$ /Thy1.1 reporter mice than in the WT counterparts (Fig. 2A). Nevertheless, phenotypic analyses of Thy1.1<sup>+</sup> CD4 T cells showed no differences in the expression of surface molecules including CD44, CD62L, CD27, and CD127 between the WT and IL-10<sup>-/-</sup> groups (Fig. 2C). These findings implicate IL-10 in regulating the magnitude but not the differentiation state of virus-specific effector CD4 T cells.

To further confirm that IL-10 has a negative impact on anti-viral CD4 T cell responses, we compared the production of Th1-associated effector cytokines by LCMV GP61-specific CD4 T cells in WT and IL-10<sup>-/-</sup> mice at day 8 following LCMV infection. We observed a marked increase in both the percentages (Fig. 3A-C) and numbers (Fig. 3D) of total IFN $\gamma$ <sup>+</sup>, IFN $\gamma$ <sup>+</sup>TNF $\alpha$ <sup>+</sup>, and IFN $\gamma$ <sup>+</sup>IL-2<sup>+</sup> LCMV-specific CD4 T cells in IL-10<sup>-/-</sup> mice compared to their WT counterparts. Notably, these elevated responses in the absence of IL-10 were not associated with altered levels of regulatory CD4 T (Treg) cells as no differences in the percentages or numbers of Treg cells was discernable between the WT and IL-10<sup>-/-</sup> groups

(Fig. 3E, F). Taken together, these data indicate that IL-10 impedes the development of anti-viral CD4 T cells which produce Th1-associated cytokines.

### **IL-10 signaling during the priming phase of infection influences the abundance and functionality of memory CD4 T cells**

To further investigate the roles of IL-10 in curtailing the development of anti-viral CD4 T cells, we treated LCMV infected WT mice with  $\alpha$ IL-10R antibodies at days 0, 2, 4, and 6 following infection, as depicted in Fig. 1A. Consistent with the results shown in Figs. 2 and 3, anti-IL-10 receptor blockade led to an enhanced anti-viral CD4 T cell response at 8 days post infection, as revealed by increased numbers of both GP66 tetramer-binding CD4 T cells and IFN $\gamma$ -producing virus-specific CD4 T cells (Fig. 4A, C, E, G). Furthermore, by 30 days post infection we detected substantially more LCMV-specific GP66 tetramer-binding and IFN $\gamma$ -producing memory CD4 T cells in the treated cohort (Fig. 4B, D, F, H). The fraction of virus-specific IFN $\gamma$ <sup>+</sup> CD4 T cells which co-produce TNF $\alpha$  or IL-2<sup>+</sup> were similar between treated and untreated mice at day 8 post infection (Fig. 4I); however, by day 30 a higher proportion of these more functional CD4 cells were detected in mice treated with  $\alpha$ IL-10R antibodies (Fig. 4J). In addition, the numbers of dual producing IFN $\gamma$ <sup>+</sup>TNF $\alpha$ <sup>+</sup> and IFN $\gamma$ <sup>+</sup>IL-2<sup>+</sup> LCMV-specific CD4 T cells were increased by the  $\alpha$ IL-10R treatment at both 8 and 30 days post infection (Fig. 4K, L). Taken together, these results further show that IL-10 signaling during the priming phase of infection negatively regulates both the quantity and functional quality of anti-viral CD4 T cell responses.

### **IL-10 negatively regulates the development of memory CD8 T cells**

The impact of IL-10 on CD4 T cell responses prompted us to investigate whether IL-10 signals also influence anti-viral CD8 T cells. To address this, WT mice were infected with LCMV and treated with  $\alpha$ IL-10R antibodies during the priming phase at days 0, 2, 4, and 6. No differences in the frequencies of LCMV GP33- and NP396-specific CD8 T cells were detected between the treated and untreated control mice at day 8 post infection (Fig. 5A-F). Nevertheless, the numbers of LCMV-specific tetramer-binding and IFN $\gamma$ -producing CD8 T cells were elevated in the treated mice due to a 1.5-fold increase in the total CD8 T cell population (Fig. 5C-F and data not shown), a phenomenon that has also been noted in  $\alpha$ IL-10R-treated and IL-10<sup>-/-</sup> mice during LCMV infections (4, 7). The expression of CD127 and KLRG1 on virus-specific CD8 T cells (Fig. 5G, H), and the ratios of CD127<sup>low</sup>KLRG1<sup>high</sup> terminal effector cells (TECs) to CD127<sup>high</sup>KLRG1<sup>low</sup> memory precursor cells (MPCs) (30) were similar between the treated and untreated cohorts (Fig. 5I). Furthermore, the levels of the transcriptional regulators Bcl6, Eomes, and T-bet in virus-specific effector CD8 T cells was also unaffected by the IL-10R blocking regimen (Fig. 5J-L). Collectively, these data indicate that IL-10 signals during the priming phase have minimal effects on the differentiation of virus-specific effector CD8 T cells during acute LCMV infection.

Consistent with the findings from the day 8 analyses (Fig. 5), we found that the  $\alpha$ IL-10R blockade increased the number but not the frequency of LCMV GP33-specific memory CD8 T cells (Fig. 6A, C) and elevated both the frequency and number of the LCMV NP396-specific population detectable at 30 days post infection (Fig. 6B, D). The frequencies and

numbers of IFN $\gamma$ -producing LCMV-specific memory CD8 T cells were also increased in mice administered  $\alpha$ IL-10R antibodies (Fig. 6E-H), and the percentages (Fig. 6I, J) and numbers (Fig. 6K, L) of anti-viral IFN $\gamma$ <sup>+</sup> CD8 T cells which co-produce TNF $\alpha$  or IL-2 were also elevated in the treated cohort compared with their untreated companions. However, by this 30 day time point the levels of Bcl6, Eomes, and T-bet, as well as the expression of CD127 and KLRG-1 were similar in both cohorts and the ratio of TEC to MPC was unaffected by the  $\alpha$ IL-10R treatment (data not shown). Taken together, these data show that IL-10 signaling during the priming phase of the response can impact both the size and functional attributes of the resulting memory CD8 T cell pool.

### Direct and indirect regulation of anti-viral CD4 T cell responses by IL-10

To compare the intrinsic (direct) and extrinsic (indirect) roles of IL-10 in regulating anti-viral CD4 T cell responses adoptive transfer studies were conducted using allelically marked LCMV-specific TCR transgenic (SMARTA) CD4 T cells (Fig. 7A). The expansion and differentiation of these cells were evaluated following LCMV infection in groups of recipients that were either left untreated or treated with  $\alpha$ IL-10R antibodies at days 0, 2, 4, and 6 following infection. Consistent with the results shown in Fig. 4, this blockade regimen enhanced the expansion of the donor SMARTA T cells as revealed by a 2.4-fold increase in the percentage ( $12.92 \pm 6.02\%$  versus  $5.34 \pm 2.55\%$ ) and a 2.5-fold increase in the number ( $1.65 \pm 1.09 \times 10^6$  versus  $0.65 \pm 0.32 \times 10^6$ ) of these donor T cells in the treated group (Fig. 7B, C). In addition, the fraction of IFN $\gamma$ -producing CD4 T cells was also boosted by inhibiting IL-10 signaling (Fig. 7D).

To further examine the roles of extrinsic IL-10 signals in modulating anti-viral CD4 T cell responses, we transferred SMARTA CD4 T cells into either WT or IL-10<sup>-/-</sup> mice and tracked the magnitude of the donor cell responses at days 7, 21, and 42 following LCMV infection (Fig. 7E). Although the differences did not reach statistical significance until day 42 post infection (Fig. 7F), the fold differences between the numbers of donor SMARTA T cells recovered from IL-10<sup>-/-</sup> and WT recipients were 2.8, 2.0, and 5.7 at days 7, 21, and 42, respectively. Since the donor SMARTA T cells were capable of producing IL-10, these results indicate that IL-10 from extrinsic sources exerted dampening effects on LCMV-specific CD4 T cell responses. Notably, the 2.8-fold difference in the number of donor SMARTA T cells at day 7 is comparable to the 2.5-fold difference we observed at day 8 when we blocked both intrinsic and extrinsic IL-10 signaling using  $\alpha$ IL-10R antibodies as shown in Fig. 7C. Taken together, these data reveal that extrinsic IL-10 signals regulate the magnitude of the virus-specific CD4 T cell response.

To define the direct and indirect effects of IL-10 on anti-viral T cell differentiation we generated mixed bone marrow chimeras reconstituted with equal numbers of allelically marked IL-10R<sup>+/+</sup> and IL-10R<sup>-/-</sup> T cell-depleted bone marrow cells (Fig. 8A). In this way, following reconstitution and infection, the IL-10R<sup>+/+</sup> and IL-10R<sup>-/-</sup> T cells are exposed to the same antigenic and environmental cues, allowing the intrinsic and extrinsic effects of IL-10 signals to be assessed. By 7 weeks following reconstitution the ratios of IL-10R<sup>-/-</sup> to IL-10R<sup>+/+</sup> CD4 and CD8 T cells in the blood were  $1.3 \pm 0.2$  and  $1.4 \pm 0.5$ , respectively and these ratios remained largely constant in the spleen following LCMV infection (data not

shown). This marginal increase in the fraction of IL-10R<sup>-/-</sup> T cells following reconstitution was mirrored by a slightly higher recovery of IL-10R<sup>-/-</sup> virus-specific CD4 (Fig. 8B) and CD8 (Fig. 8C) T cells at 8 days following infection. By 30 days following infection, however, the recoveries of virus-specific IL-10R<sup>+/+</sup> and IL-10R<sup>-/-</sup> T cells were comparable (Fig. 8B, C) and other phenotypic attributes were similar, including the production of IFN $\gamma$ , TNF $\alpha$ , and IL-2, the levels of the Bcl6, and T-bet (by both CD4 and CD8 T cells), as well as Eomes and the ratios of CD127<sup>low</sup> KLRG-1<sup>high</sup> (TECs) to CD127<sup>high</sup> KLRG-1<sup>low</sup> (MPCs) for CD8 T cells (data not shown). Taken together with the day 8 findings, these results suggest that IL-10 may play a subtle, direct pro-survival role during the contraction phase.

To examine whether IL-10 directly influences the differentiation of virus-specific Th1 and Tfh cells, we analyzed the expression of CXCR5 and signaling lymphocytic activation molecule (SLAM) on IL-10R<sup>+/+</sup> to IL-10R<sup>-/-</sup> GP66-specific CD4 T cells. Th1 cells are predominantly CXCR5<sup>low</sup>SLAM<sup>high</sup>, whereas Tfh cells are CXCR5<sup>high</sup>SLAM<sup>low</sup> (31). The absence of IL-10 signaling in CD4 T cells very modestly increased the frequency and number of virus-specific Th1 cells, resulting in an increased ratio of Th1 to Tfh cells at 8 days following infection (Fig. 8D, F). At this time point the frequency of IL-10R<sup>-/-</sup> Tfh cells was also reduced, although the absolute numbers were not (Fig. 8D, F). These differences in the frequencies, numbers, and ratios of Th1 and Tfh CD8 T cells were, however, not sustained by day 30 post infection (Fig. 8E, G). Furthermore, IL-10R<sup>+/+</sup> and IL-10R<sup>-/-</sup> virus-specific CD4 T cells displayed similar patterns of PD-1, P-selectin glycoprotein ligand 1 (PSGL1) and Ly6C expression as well as T-bet and Bcl6 (data not shown), suggesting that the role of direct IL-10 signaling on CD4 T cell differentiation may be limited. Taken together, these data indicate that IL-10 does not act directly on T cells to substantially dictate the differentiation state and function of Th1, Tfh, and CD8 T cells following acute LCMV infection but may act directly to subtly promote the overall magnitude of the response.

### IL-10 modulates the balance between anti-viral Th1 and Tfh responses

Our evaluation of IL-10R<sup>+/+</sup> and IL-10R<sup>-/-</sup> mixed bone marrow chimeras revealed that IL-10 does not play a substantial role in directly regulating LCMV-specific T cell responses (Fig. 8). Nevertheless, IL-10R blockade treatments did imply that IL-10 indirectly influences the magnitude and functional properties of anti-viral T cells (Figs. 4–7). Therefore, we revisited these blockade studies to more comprehensively dissect how IL-10 influences CD4 T cell differentiation during acute LCMV infection. Cohorts of WT mice were either left untreated or treated with  $\alpha$ IL-10R antibodies, as in Fig. 1A and LCMV GP66-specific CD4 T cells and Treg cells were identified by staining with I-A<sup>b</sup> GP66 tetramers and anti-Foxp3 antibodies, respectively. The expression of CXCR5 and PD-1 by these cells was then scrutinized to differentiate between LCMV GP66-specific Tfh cells (CD4<sup>+</sup>CD19<sup>-</sup>GP66<sup>+</sup>Foxp3<sup>-</sup>CXCR5<sup>high</sup>PD-1<sup>high</sup>) and Tfr cells (CD4<sup>+</sup>CD19<sup>-</sup>GP66<sup>-</sup>Foxp3<sup>+</sup>CXCR5<sup>high</sup>PD-1<sup>high</sup>) (Fig. 9A). Notably, we did not detect LCMV-specific Treg cells (Fig. 9A), which is consistent with previous reports (32). Anti-IL-10R blockade reduced the frequencies but not overall numbers of GP66<sup>+</sup> Tfh cells detectable at days 8 and 30 following infection (Fig. 9B, D, F). This discrepancy is accounted for by the increase in the overall size of the GP66-specific response detectable in the treated mice (Fig. 4C, D). A minor reduction in the percentage of Tfr cells was observed at day 8 post infection (Fig. 9C,

E), however this difference did not reach statistical significance and was not sustained by day 30 post infection (Fig. 9G). Notably, as depicted in Fig. 9H, the ratio of IFN $\gamma$ -producing virus-specific CD4 T cells to GP66<sup>+</sup> Tfh cells was increased by the  $\alpha$ IL-10R blockade particularly at day 30 post infection ( $6.5\pm 1.5$  versus  $4.6\pm 1.3$  and  $17.2\pm 3.7$  versus  $6.6\pm 2.3$  at day 8 and day 30, respectively). Moreover, IFN $\gamma$ <sup>+</sup> virus-specific CD4 T cells predominantly adopted a CXCR5<sup>low</sup>SLAM<sup>high</sup> Th1 phenotype ( $88\pm 4\%$  and  $88\pm 3\%$  in WT and  $\alpha$ IL-10R-treated mice, respectively) (Fig. 9I). These findings indicate that IL-10 acts to dampen anti-viral Th1 differentiation while permitting the generation of Tfh responses during acute LCMV infections.

To verify the impact of IL-10R blockade on virus-specific Th1 and Tfh responses, we analyzed the expression of CXCR5 and SLAM on GP66 tetramer-binding CD4 T cells. Although only a modest increase in the numbers of GP66-specific SLAM<sup>high</sup> CXCR5<sup>low</sup> Th1 cells were detectable in the treated cohort at 8 days following infection (Fig. 10A, C), by day 30 the differences were more pronounced and a greater fraction and number of Th1 cells were detected, resulting a higher Th1:Tfh cell ratio (Fig. 10B, D). In order to further confirm these findings, we used PSGL1 and Ly6C to discriminate Th1 and Tfh cells. PSGL1<sup>high</sup>Ly6C<sup>high</sup> and PSGL1<sup>low</sup>Ly6C<sup>low</sup> virus-specific CD4 T cells are predominantly Th1 and Tfh cells, respectively, while PSGL1<sup>high</sup>Ly6C<sup>low</sup> cells may contain a mixture of Th1 and Tfh populations (31, 33, 34). Consistent with the CXCR5 and SLAM costaining results, the frequency but not the number of GP66-specific PSGL1<sup>low</sup>Ly6C<sup>low</sup> Tfh cells was substantially reduced in the  $\alpha$ IL-10R-treated cohorts and conversely the percentage and number of PSGL1<sup>high</sup>Ly6C<sup>high</sup> Th1 cells were elevated (Fig. 10E-H). Consequently, the ratios of PSGL1<sup>high</sup>Ly6C<sup>high</sup> Th1 to PSGL1<sup>low</sup>Ly6C<sup>low</sup> Tfh cells were increased in the treated mice at both 8 and 30 days following infection (Fig. 10E, F).

Although the expression of the transcription factors T-bet and Bcl6 in virus-specific CD4 T cell populations was largely similar between treated and untreated control mice at day 8 post infection (data not shown), the  $\alpha$ IL-10R blockade modestly elevated the levels of T-bet (Fig. 10I), and slightly reduced the levels of Bcl6 (Fig. 10J) in GP66-specific CD4 T cells at 30 days post infection. Since T-bet and Bcl6 foster the differentiation programs of Th1 and Tfh cells, respectively (35), these results together with the data shown in Figs. 4 and 9 demonstrate that IL-10 can influence the differentiation states of virus-specific Th1 and Tfh cells via indirect T cell-extrinsic mechanisms. Collectively, our results demonstrate that IL-10 signals during the priming phase of infection does not regulate the humoral immune response against LCMV infection, as both GC B cell and antibody responses were largely unaffected by the  $\alpha$ IL-10R blockade; however, IL-10 acts indirectly to modulate the balance of anti-viral Th1 and Tfh cell responses.

## Discussion

This study reveals several important roles for IL-10 in regulating immune responses during a prototypic acute viral infection. First, IL-10 restricts the magnitude of effector and memory Th1 responses. This is shown by increased numbers of IFN $\gamma$ -producing virus-specific CD4 T cells in IL-10<sup>-/-</sup> mice as well as in mice that received  $\alpha$ IL-10R blockade; furthermore, an increased fraction of virus-specific CXCR5<sup>low</sup>SLAM<sup>high</sup> as well as PSGL1<sup>high</sup>Ly6C<sup>high</sup> Th1

phenotype CD4 cells are detected when IL-10 signals are blocked. Second, IL-10 production by virus-specific CD4 T cells themselves is not sufficient to limit their expansion and maintenance following acute viral infection. Third, IL-10 signaling during the priming phase of the response reduces the formation of memory CD8 T cells as blockade of IL-10 signaling during this time period leads to increased numbers of virus-specific memory CD8 T cells. Fourth, IL-10 influences the functional quality of memory CD4 and CD8 T cells. This is clearly shown by higher proportions of IFN $\gamma$ <sup>+</sup> virus-specific memory CD4 and CD8 T cells that can co-produce TNF $\alpha$  or IL-2 in mice treated with  $\alpha$ IL-10R antibodies. Fifth, the effects of IL-10 on T cell differentiation and functionality are largely mediated by indirect T cell-extrinsic mechanisms as evidenced by generally comparable IL-10R<sup>+/+</sup> and IL-10R<sup>-/-</sup> anti-viral T cell responses following LCMV infection of mixed bone marrow chimeras. Finally, IL-10 influences the balance between Th1 and Tfh cell development, which is demonstrated by the reduced frequency of virus-specific Tfh cells and increased ratio of Th1 to Tfh cells when IL-10 signaling is blocked. Collectively, our results show that IL-10 exerts suppressive effects on the development and functional maturation of memory CD4 and CD8 T cells as well as the balance of anti-viral Th1 and Tfh cells following acute viral infection.

Consistent with a previous report (7), this study further demonstrates that IL-10 controls the development of effector and memory Th1 cells after an acute viral infection. Nevertheless, while the studies by Brooks *et al.*, (7) suggest that IL-10 suppresses the differentiation of effector and memory CD4 T cells in a cell-intrinsic manner, our studies indicate that IL-10 largely functions indirectly on CD4 T cells to restrict anti-viral Th1 responses. It is possible that this is due to differences between the adoptive transfer strategies using T cell receptor transgenic CD4 T cells versus the mixed bone marrow chimeras used in this study. Thus, several parameters likely differ between these systems including the frequencies of virus-specific CD4 and CD8 T cells, the clonality of the response, and kinetics of viral clearance.

Several studies have shown that virus-specific CD4 T cells produce IL-10 during chronic LCMV infection (3, 4, 36, 37) and may therefore be self-regulatory (36, 37); however, our data suggest that following acute LCMV infection the production of IL-10 by virus-specific CD4 T cells has minimal effects on controlling Th1 responses. Other cell types including dendritic cells, monocytes, and Treg cells are possible cellular sources of IL-10 (3, 4, 36). The environmental differences between acute and chronic viral infections such as antigenic and inflammatory signals may account for this discrepancy, and therefore further studies are needed to identify the physiologically relevant producers of IL-10 following acute LCMV infection.

In this study, we identified IL-10 as a factor that can act indirectly to regulate the balance between Th1 and Tfh cells. IL-10 signaling during the priming phase of infection limits the generation of Th1 cells, while increasing the frequency but not the number of Tfh cells. As a result, the relative abundance of Th1 cells compared to Tfh cells was higher, especially by 30 days post infection, when IL-10 signals were blocked during the priming phase. Additionally, early IL-10 signals may dictate the differentiation states of memory Th1 and Tfh cells as revealed by increased T-bet and decreased Bcl6 expression when IL-10 signals were blocked during the priming phase of infection. Interestingly, our mixed bone marrow

chimera studies indicate that the actions of IL-10 signals on Th1 and Tfh cell differentiation are T cell-extrinsic. Although further studies will be necessary to define how IL-10 indirectly regulates anti-viral CD4 and CD8 T cell responses, we speculate that alterations in the levels of other cytokines, which may occur if IL-10 signals are ablated, and/or IL-10-dependent changes in the activation state and properties of professional antigen-presenting cells may influence the outcome of the response.

Despite the elevated ratio of Th1 cells to Tfh cells, we did not observe any difference in GC B cell or LCMV-specific antibody responses in the absence of IL-10 signaling during the priming phase of infection. Although this does not rule out the possibility that IL-10 regulates the resolution and/or maintenance of GCs at later stages, our results are consistent with previous studies indicating that anti-viral antibody responses are not altered in IL-10<sup>-/-</sup> mice or by the  $\alpha$ IL-10R treatment in the setting of chronic LCMV infection (3, 4). Notably, IL-10 has been reported to both positively and negatively regulate GC B and antibody responses under certain conditions (5, 28, 29, 38–42). Thus, the role of IL-10 in GC reactions is likely context-dependent.

Depending on the experimental systems used, IL-10 can promote, suppress or have little impact on the differentiation of memory CD8 T cells (3, 4, 7, 8, 14–17). The suppressive effects of IL-10 on CD8 T cell responses have been reported during viral and bacterial infections in mice and humans (3–5, 8–10). Here, our study provides another line of evidence that IL-10 signaling during the priming phase acts indirectly to restrict the formation of LCMV-specific memory CD8 T cells and limits their functional maturation. It has also been reported that during acute LCMV infection IL-10 acts during the early contraction phase of the response, between days 8 to 15 post infection, but not during the priming phase (days 0 to 8), to promote the formation of CD127<sup>high</sup>KLRG1<sup>low</sup>CD62L<sup>high</sup> central memory CD8 T cells (15); however, whether IL-10 influences cytokine production by virus-specific CD8 T cells was not assessed in that study. Additionally, the anti-IL-10 antibody used in that study may have a different half-life and/or potency than the anti-IL-10 receptor blockade strategy used in this report. Blocking the IL-10 receptor at day 0 and day 5 during acute LCMV infection has also been suggested to have minimal effects on the antiviral CD8 T cell response (7). Nevertheless, the timing of antibody administration and also the route and dose of LCMV infection differed from those used in our study, which may alter the availability of viral antigens and pace of viral clearance. It is plausible that the kinetics and strength of antigenic signals modulate the impact of IL-10 and/or IL-10-induced signals on CD8 T cell responses. Indeed, we observed that IL-10-associated signals more potently suppress LCMV NP396-specific CD8 T cells than those reactive against the GP33 epitope. It has been shown that the NP396 epitope is presented earlier than the GP33 epitope following infection, which results in faster activation of NP396-specific CD8 T cells (43–45). In addition, by comparison with LCMV GP33-specific CD8 T cells, lower frequencies of NP396-specific CD8 T cells are present in unimmunized mice (46). Thus, NP396-specific CD8 T cells may receive earlier and stronger T cell receptor (TCR) signaling and we speculate that this renders NP396-specific CD8 T cells more sensitive to IL-10-induced suppressive signals than their GP33-specific counterparts.

In summary, our data demonstrate that IL-10 plays a suppressive role in the development of memory CD4 and CD8 T cells and provide rationale for the deliberate inhibition of IL-10 signaling in order to enhance the formation and functionality of memory T cells elicited by natural infections or vaccination. In addition, manipulating IL-10 or IL-10 signaling may enable the developing CD4 T cell response to be directed towards or away from Th1 development to promote infection control or to attenuate pathogenic responses.

## Acknowledgments

We thank Davide Botta for technical assistance, as well as the members of the Harrington and Zajac laboratories for their help and critical reading of this manuscript.

This work was supported in part by grants AI049360 and AI109962 (to A.J.Z), DK08408 and AI113007 (to L.E.H), and AI07051 to (SBM) from the National Institutes of Health.

## References

- Ouyang W, Rutz S, Crellin NK, Valdez PA, Hymowitz SG. Regulation and functions of the IL-10 family of cytokines in inflammation and disease. *Annu. Rev. Immunol.* 2011; 29:71–109. [PubMed: 21166540]
- Cox MA, Kahan SM, Zajac AJ. Anti-viral CD8 T cells and the cytokines that they love. *Virology.* 2013; 435:157–169. [PubMed: 23217625]
- Brooks DG, Trifilo MJ, Edelmann KH, Teyton L, McGavern DB, Oldstone MB. Interleukin-10 determines viral clearance or persistence in vivo. *Nat. Med.* 2006; 12:1301–1309. [PubMed: 17041596]
- Ejrnaes M, Filippi CM, Martinic MM, Ling EM, Togher LM, Crotty S, von Herrath MG. Resolution of a chronic viral infection after interleukin-10 receptor blockade. *J. Exp. Med.* 2006; 203:2461–2472. [PubMed: 17030951]
- Maris CH, Chappell CP, Jacob J. Interleukin-10 plays an early role in generating virus-specific T cell anergy. *BMC Immunol.* 2007; 8:8. [PubMed: 17570849]
- Richter K, Perriard G, Oxenius A. Reversal of chronic to resolved infection by IL-10 blockade is LCMV strain dependent. *Eur. J. Immunol.* 2013; 43:649–654. [PubMed: 23348876]
- Brooks DG, Walsh KB, Elsaesser H, Oldstone MB. IL-10 directly suppresses CD4 but not CD8 T cell effector and memory responses following acute viral infection. *Proc. Natl. Acad. Sci. U. S. A.* 2010; 107:3018–3023. [PubMed: 20133700]
- Biswas PS, Pedicord V, Ploss A, Menet E, Leiner I, Pamer EG. Pathogen-specific CD8 T cell responses are directly inhibited by IL-10. *J. Immunol.* 2007; 179:4520–4528. [PubMed: 17878348]
- Brockman MA, Kwon DS, Tighe DP, Pavlik DF, Rosato PC, Sela J, Porichis F, Le Gall S, Waring MT, Moss K, Jessen H, Pereyra F, Kavanagh DG, Walker BD, Kaufmann DE. IL-10 is up-regulated in multiple cell types during viremic HIV infection and reversibly inhibits virus-specific T cells. *Blood.* 2009; 114:346–356. [PubMed: 19365081]
- Clerici M, Wynn TA, Berzofsky JA, Blatt SP, Hendrix CW, Sher A, Coffman RL, Shearer GM. Role of interleukin-10 in T helper cell dysfunction in asymptomatic individuals infected with the human immunodeficiency virus. *J. Clin. Invest.* 1994; 93:768–775. [PubMed: 8113410]
- Brooks DG, Lee AM, Elsaesser H, McGavern DB, Oldstone MB. IL-10 blockade facilitates DNA vaccine-induced T cell responses and enhances clearance of persistent virus infection. *J. Exp. Med.* 2008; 205:533–541. [PubMed: 18332180]
- Brooks DG, Ha SJ, Elsaesser H, Sharpe AH, Freeman GJ, Oldstone MB. IL-10 and PD-L1 operate through distinct pathways to suppress T-cell activity during persistent viral infection. *Proc. Natl. Acad. Sci. U. S. A.* 2008; 105:20428–20433. [PubMed: 19075244]
- Freeman BE, Meyer C, Slifka MK. Anti-inflammatory cytokines directly inhibit innate but not adaptive CD8+ T cell functions. *J. Virol.* 2014; 88:7474–7484. [PubMed: 24741101]

14. Cui W, Liu Y, Weinstein JS, Craft J, Kaech SM. An interleukin-21-interleukin-10-STAT3 pathway is critical for functional maturation of memory CD8+ T cells. *Immunity*. 2011; 35:792–805. [PubMed: 22118527]
15. Laidlaw BJ, Cui W, Amezquita RA, Gray SM, Guan T, Lu Y, Kobayashi Y, Flavell RA, Kleinstein SH, Craft J, Kaech SM. Production of IL-10 by CD4(+) regulatory T cells during the resolution of infection promotes the maturation of memory CD8(+) T cells. *Nat. Immunol.* 2015; 16:871–879. [PubMed: 26147684]
16. Foulds KE, Rotte MJ, Seder RA. IL-10 is required for optimal CD8 T cell memory following *Listeria monocytogenes* infection. *J. Immunol.* 2006; 177:2565–2574. [PubMed: 16888018]
17. Kang SS, Allen PM. Priming in the presence of IL-10 results in direct enhancement of CD8+ T cell primary responses and inhibition of secondary responses. *J. Immunol.* 2005; 174:5382–5389. [PubMed: 15843536]
18. Crotty S. Follicular helper CD4 T cells (TFH). *Annu. Rev. Immunol.* 2011; 29:621–663. [PubMed: 21314428]
19. Chung Y, Tanaka S, Chu F, Nurieva RI, Martinez GJ, Rawal S, Wang YH, Lim H, Reynolds JM, Zhou XH, Fan HM, Liu ZM, Neelapu SS, Dong C. Follicular regulatory T cells expressing Foxp3 and Bcl-6 suppress germinal center reactions. *Nat. Med.* 2011; 17:983–988. [PubMed: 21785430]
20. Linterman MA, Pierson W, Lee SK, Kallies A, Kawamoto S, Rayner TF, Srivastava M, Divekar DP, Beaton L, Hogan JJ, Fagarasan S, Liston A, Smith KG, Vinuesa CG. Foxp3+ follicular regulatory T cells control the germinal center response. *Nat. Med.* 2011; 17:975–982. [PubMed: 21785433]
21. Wollenberg I, Agua-Doce A, Hernandez A, Almeida C, Oliveira VG, Faro J, Graca L. Regulation of the germinal center reaction by Foxp3+ follicular regulatory T cells. *J. Immunol.* 2011; 187:4553–4560. [PubMed: 21984700]
22. Harrington LE, Janowski KM, Oliver JR, Zajac AJ, Weaver CT. Memory CD4 T cells emerge from effector T-cell progenitors. *Nature*. 2008; 452:356–360. [PubMed: 18322463]
23. Ahmed R, Salmi A, Butler LD, Chiller JM, Oldstone MB. Selection of genetic variants of lymphocytic choriomeningitis virus in spleens of persistently infected mice. Role in suppression of cytotoxic T lymphocyte response and viral persistence. *J. Exp. Med.* 1984; 160:521–540. [PubMed: 6332167]
24. Tian Y, Cox MA, Kahan SM, Ingram JT, Bakshi RK, Zajac AJ. A Context-Dependent Role for IL-21 in Modulating the Differentiation, Distribution, and Abundance of Effector and Memory CD8 T Cell Subsets. *J. Immunol.* 2016; 196:2153–2166. [PubMed: 26826252]
25. Fuller MJ, Zajac AJ. Ablation of CD8 and CD4 T cell responses by high viral loads. *J. Immunol.* 2003; 170:477–486. [PubMed: 12496434]
26. Arpin C, Dechanet J, Van Kooten C, Merville P, Grouard G, Briere F, Banchereau J, Liu YJ. Generation of memory B cells and plasma cells in vitro. *Science*. 1995; 268:720–722. [PubMed: 7537388]
27. Choe J, Choi YS. IL-10 interrupts memory B cell expansion in the germinal center by inducing differentiation into plasma cells. *Eur. J. Immunol.* 1998; 28:508–515. [PubMed: 9521060]
28. Chacon-Salinas R, Limon-Flores AY, Chavez-Blanco AD, Gonzalez-Estrada A, Ullrich SE. Mast cell-derived IL-10 suppresses germinal center formation by affecting T follicular helper cell function. *J. Immunol.* 2011; 186:25–31. [PubMed: 21098222]
29. Wu HY, Quintana FJ, Weiner HL. Nasal anti-CD3 antibody ameliorates lupus by inducing an IL-10-secreting CD4+ CD25– LAP+ regulatory T cell and is associated with down-regulation of IL-17+ CD4+ ICOS+ CXCR5+ follicular helper T cells. *J. Immunol.* 2008; 181:6038–6050. [PubMed: 18941193]
30. Kaech SM, Cui W. Transcriptional control of effector and memory CD8+ T cell differentiation. *Nat. Rev. Immunol.* 2012; 12:749–761. [PubMed: 23080391]
31. Choi YS, Yang JA, Yusuf I, Johnston RJ, Greenbaum J, Peters B, Crotty S. Bcl6 expressing follicular helper CD4 T cells are fate committed early and have the capacity to form memory. *J. Immunol.* 2013; 190:4014–4026. [PubMed: 23487426]

32. Punkosdy GA, Blain M, Glass DD, Lozano MM, O'Mara L, Dudley JP, Ahmed R, Shevach EM. Regulatory T-cell expansion during chronic viral infection is dependent on endogenous retroviral superantigens. *Proc. Natl. Acad. Sci. U. S. A.* 2011; 108:3677–3682. [PubMed: 21321220]
33. Marshall HD, Chandele A, Jung YW, Meng H, Poholek AC, Parish IA, Rutishauser R, Cui W, Kleinstein SH, Craft J, Kaech SM. Differential expression of Ly6C and T-bet distinguish effector and memory Th1 CD4(+) cell properties during viral infection. *Immunity.* 2011; 35:633–646. [PubMed: 22018471]
34. Hale JS, Youngblood B, Latner DR, Mohammed AU, Ye L, Akondy RS, Wu T, Iyer SS, Ahmed R. Distinct memory CD4+ T cells with commitment to T follicular helper- and T helper 1-cell lineages are generated after acute viral infection. *Immunity.* 2013; 38:805–817. [PubMed: 23583644]
35. Tripathi SK, Lahesmaa R. Transcriptional and epigenetic regulation of T-helper lineage specification. *Immunol. Rev.* 2014; 261:62–83. [PubMed: 25123277]
36. Parish IA, Marshall HD, Staron MM, Lang PA, Brustle A, Chen JH, Cui W, Tsui YC, Perry C, Laidlaw BJ, Ohashi PS, Weaver CT, Kaech SM. Chronic viral infection promotes sustained Th1-derived immunoregulatory IL-10 via BLIMP-1. *J. Clin. Invest.* 2014; 124:3455–3468. [PubMed: 25003188]
37. Richter K, Perriard G, Behrendt R, Schwendener RA, Sexl V, Dunn R, Kamanaka M, Flavell RA, Roers A, Oxenius A. Macrophage and T cell produced IL-10 promotes viral chronicity. *PLoS Pathog.* 2013; 9:e1003735. [PubMed: 24244162]
38. Sun K, Torres L, Metzger DW. A detrimental effect of interleukin-10 on protective pulmonary humoral immunity during primary influenza A virus infection. *J. Virol.* 2010; 84:5007–5014. [PubMed: 20200252]
39. Cai G, Nie X, Zhang W, Wu B, Lin J, Wang H, Jiang C, Shen Q. A regulatory role for IL-10 receptor signaling in development and B cell help of T follicular helper cells in mice. *J. Immunol.* 2012; 189:1294–1302. [PubMed: 22753938]
40. Levy Y, Brouet JC. Interleukin-10 prevents spontaneous death of germinal center B cells by induction of the bcl-2 protein. *J. Clin. Invest.* 1994; 93:424–428. [PubMed: 8282815]
41. Marcelletti JF, Katz DH. IL-10 stimulates murine antigen-driven antibody responses in vitro by regulating helper cell subset participation. *Cell. Immunol.* 1996; 167:86–98. [PubMed: 8548850]
42. De Winter H, Elewaut D, Turovskaya O, Huflejt M, Shimeld C, Hagenbaugh A, Binder S, Takahashi I, Kronenberg M, Cheroutre H. Regulation of mucosal immune responses by recombinant interleukin 10 produced by intestinal epithelial cells in mice. *Gastroenterology.* 2002; 122:1829–1841. [PubMed: 12055591]
43. Probst HC, Tschannen K, Gallimore A, Martinic M, Basler M, Dumrese T, Jones E, van den Broek MF. Immunodominance of an antiviral cytotoxic T cell response is shaped by the kinetics of viral protein expression. *J. Immunol.* 2003; 171:5415–5422. [PubMed: 14607945]
44. Bruns M, Kratzberg T, Zeller W, Lehmann-Grube F. Mode of replication of lymphocytic choriomeningitis virus in persistently infected cultivated mouse L cells. *Virology.* 1990; 177:615–624. [PubMed: 1695411]
45. Tebo AE, Fuller MJ, Gaddis DE, Kojima K, Rehani K, Zajac AJ. Rapid recruitment of virus-specific CD8 T cells restructures immunodominance during protective secondary responses. *J. Virol.* 2005; 79:12703–12713. [PubMed: 16188973]
46. Obar JJ, Khanna KM, Lefrancois L. Endogenous naive CD8+ T cell precursor frequency regulates primary and memory responses to infection. *Immunity.* 2008; 28:859–869. [PubMed: 18499487]

### Abbreviations used in this paper

<b>GC</b>	germinal center
<b>LCMV</b>	lymphocytic choriomeningitis virus
<b>MFI</b>	mean fluorescence intensity

<b>MPC</b>	memory precursor cell
<b>TEC</b>	terminal effector cell
<b>Tfh</b>	follicular helper T cell
<b>Tfr</b>	follicular regulatory T cell
<b>Th1</b>	type 1 helper T cell
<b>Treg</b>	regulatory T cell

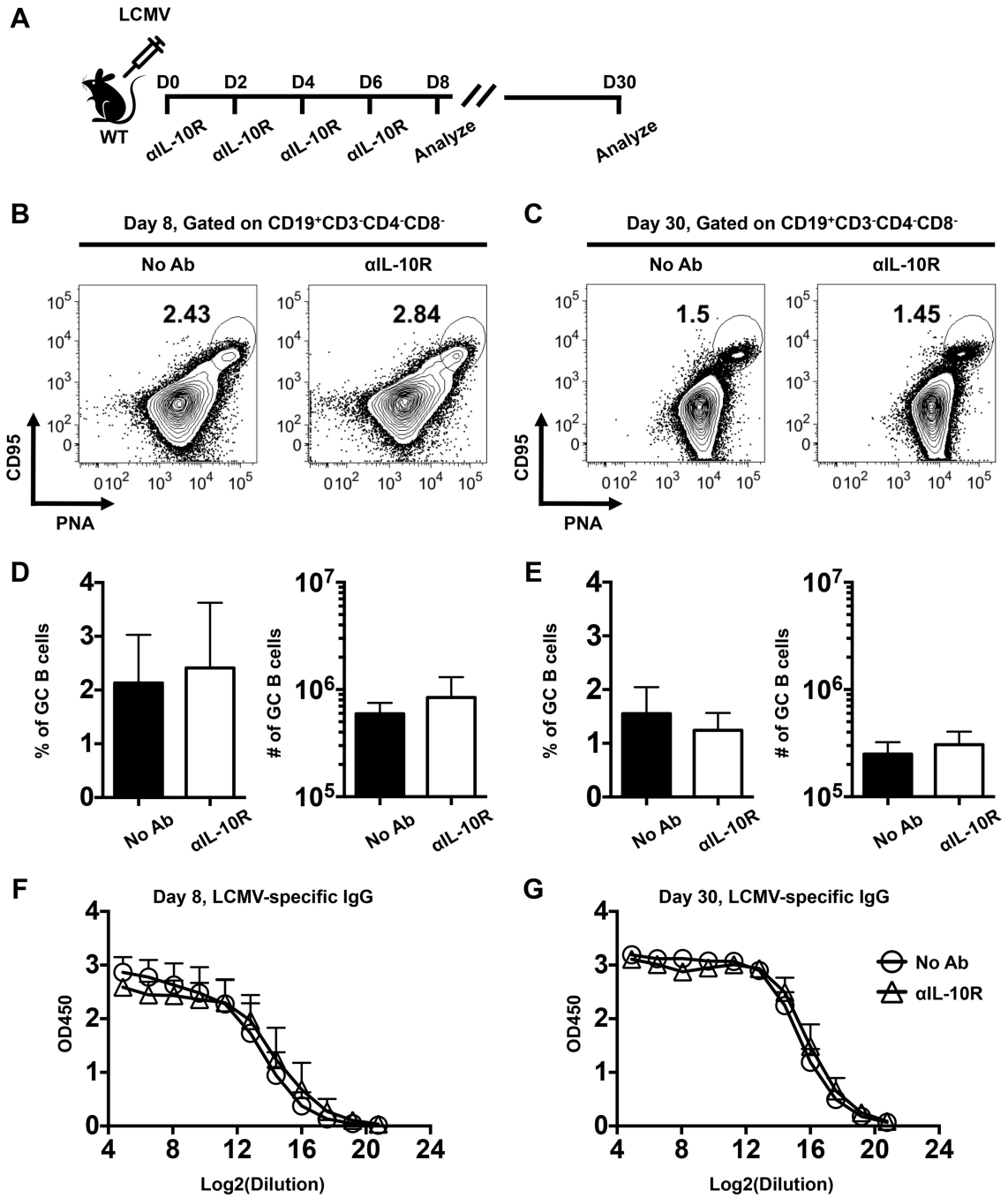


**FIGURE 1.**

GC B cell and antibody responses develop independently of IL-10. (A) Schematic depicting the experimental set-up. WT mice were either left untreated or treated with anti-IL-10 receptor (αIL-10R) antibodies at days 0, 2, 4, and 6 following LCMV infection. GC B cell and LCMV-specific antibody responses were then analyzed at days 8 and 30. (B-C) Representative contour plots show gated CD19<sup>+</sup>CD3<sup>-</sup>CD4<sup>-</sup>CD8<sup>-</sup> B cells in the spleens of infected mice at (B) 8 or (C) 30 days following infection. The percentages of CD95<sup>+</sup>PNA<sup>+</sup> GC B cells are indicated. (D-E) Bar graphs show the percentages (left panels) or numbers

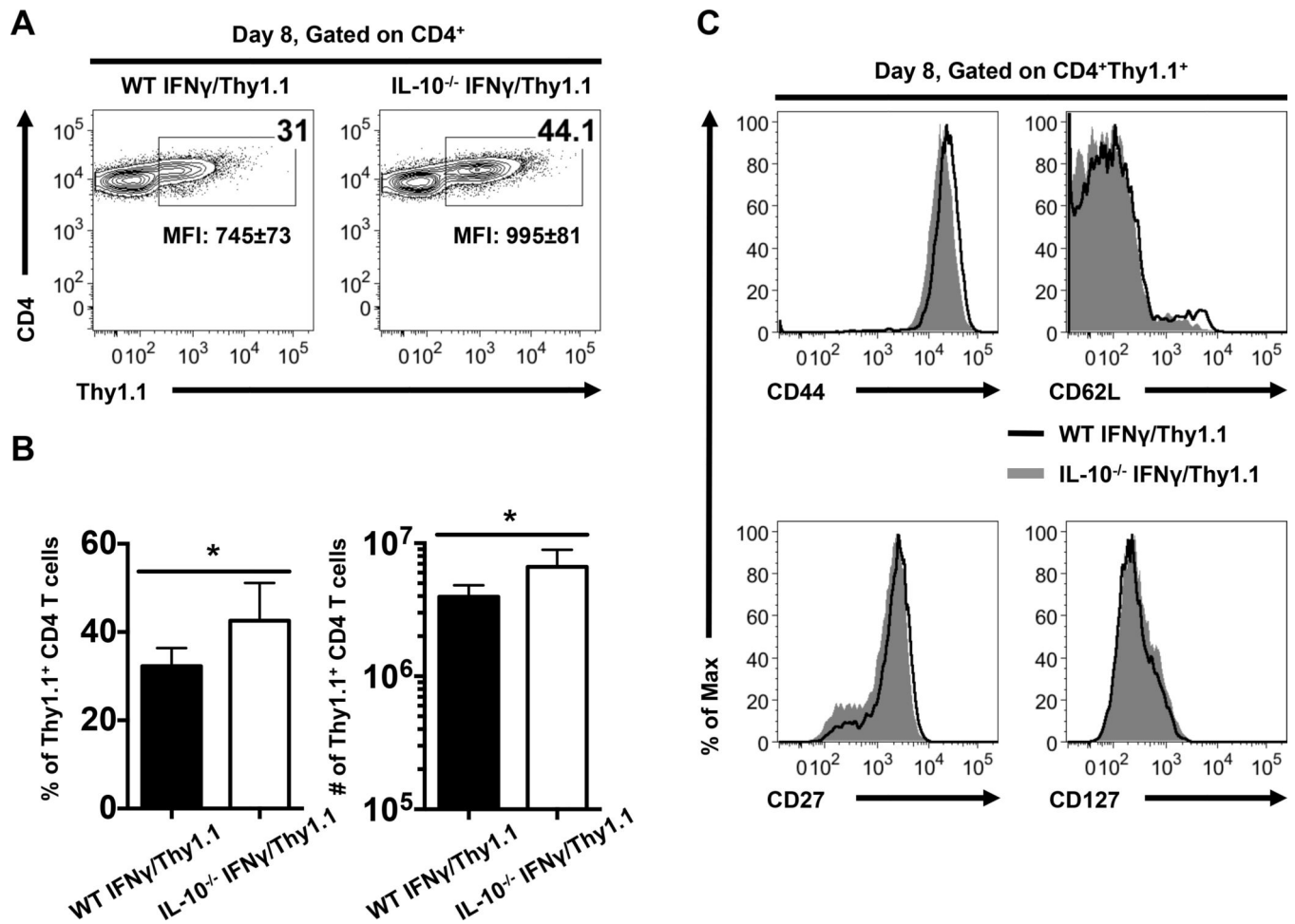
(right panels) of GC B cells at **(D)** day 8 or **(E)** day 30 following infection. **(F-G)** LCMV-specific serum IgG titers were analyzed at **(F)** 8 and **(G)** 30 days post infection. Composite results from two independent experiments are presented with 9–10 mice per group. Error bars show SD.

Author Manuscript

Author Manuscript

Author Manuscript

Author Manuscript

**FIGURE 2.**

Increased expansion of anti-viral Th1 cells in IL-10<sup>-/-</sup> IFN $\gamma$ /Thy1.1 reporter mice. (A) Representative contour plots show *ex vivo* Thy1.1 (the IFN $\gamma$  reporter molecule) expression by splenic CD4 T cells at 8 days following LCMV infection of WT and IL-10<sup>-/-</sup> IFN $\gamma$ /Thy1.1 mice. Numbers indicate the percentages or MFI  $\pm$  SD of Thy1.1 expression by CD4 T cells. (B) Bar graphs show the percentages (left panel) or numbers (right panel) of Thy1.1<sup>+</sup> CD4 T cells with error bars indicating SD. (C) Representative histograms show the expression of CD44, CD62L, CD27, and CD127 on gated Thy1.1<sup>+</sup> CD4 T cells. Representative or composite data are shown from two independent experiments with 4–5 mice per group. \* $p < 0.05$ .

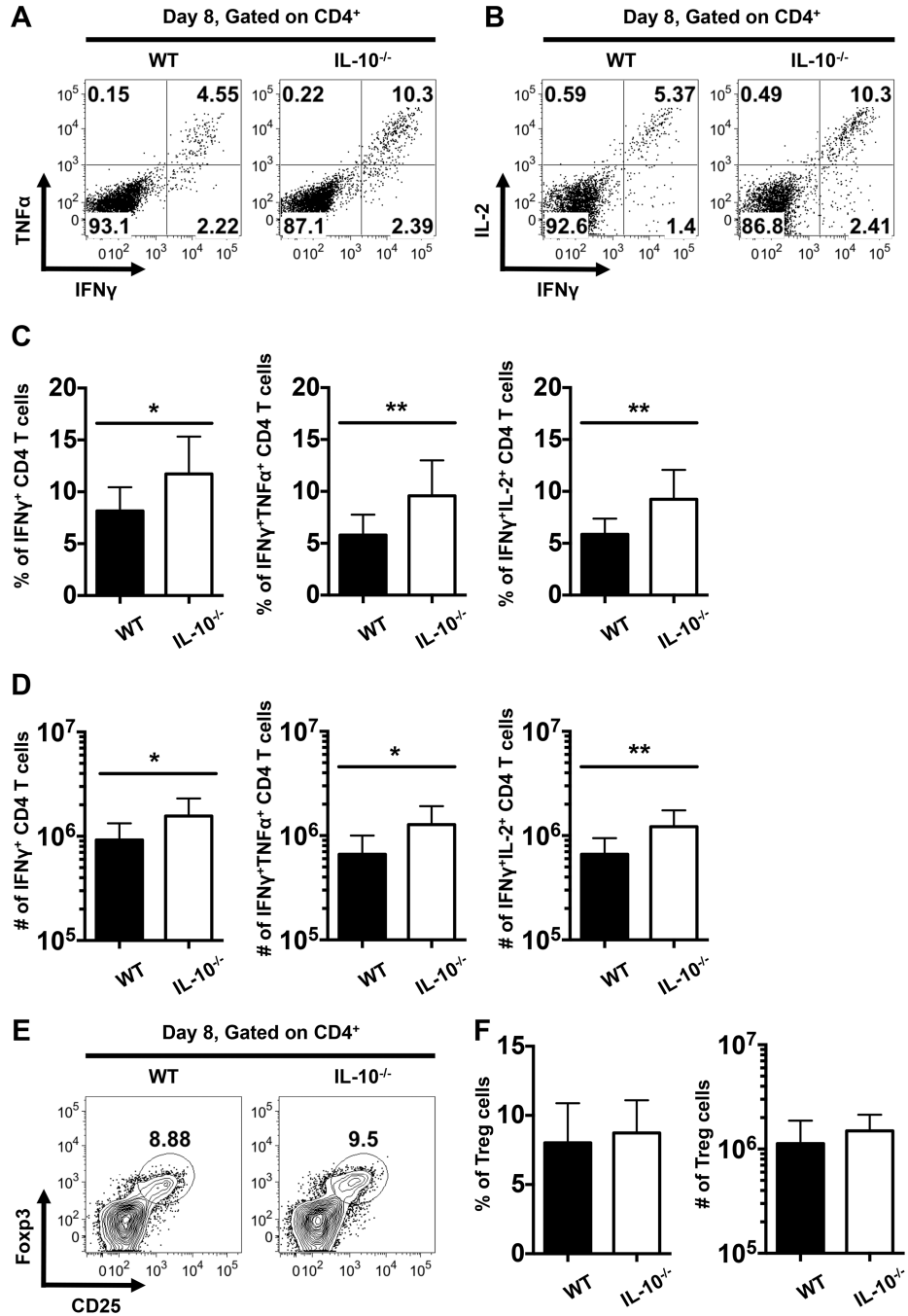


**FIGURE 3.** Enhanced magnitude of LCMV-specific CD4 T cell responses in IL-10<sup>-/-</sup> mice following acute LCMV infection. (A-D) Splenocytes from LCMV infected WT and IL-10<sup>-/-</sup> mice were stimulated with the LCMV GP61-80 peptide and intracellular staining was performed to evaluate the production of IFN $\gamma$ , TNF $\alpha$ , and IL-2 at day 8 following infection. (A-B) Representative dot plots show the production of IFN $\gamma$  and either (A) TNF $\alpha$  or (B) IL-2 by gated CD4 T cells. (C-D) Bar graphs show the (C) percentages or (D) numbers of cytokine-producing CD4 T cells. In (A-D), representative or composite data are shown from two

independent experiments analyzing eleven mice per group. **(E)** Representative contour plots show the expression of Foxp3 and CD25 on gated splenic CD4 T cells at 8 days following LCMV infection of WT and IL-10<sup>-/-</sup> mice. Numbers indicate the percentages of Foxp3<sup>+</sup>CD25<sup>+</sup> Treg cells. **(F)** Bar graphs show the percentages (left panel) or numbers (right panel) of Treg cells. In **(E)** and **(F)**, representative or composite data are shown from two independent experiments analyzing six mice per group. \* $p < 0.05$ , \*\* $p < 0.01$ . Error bars show SD.

Author Manuscript

Author Manuscript

Author Manuscript

Author Manuscript

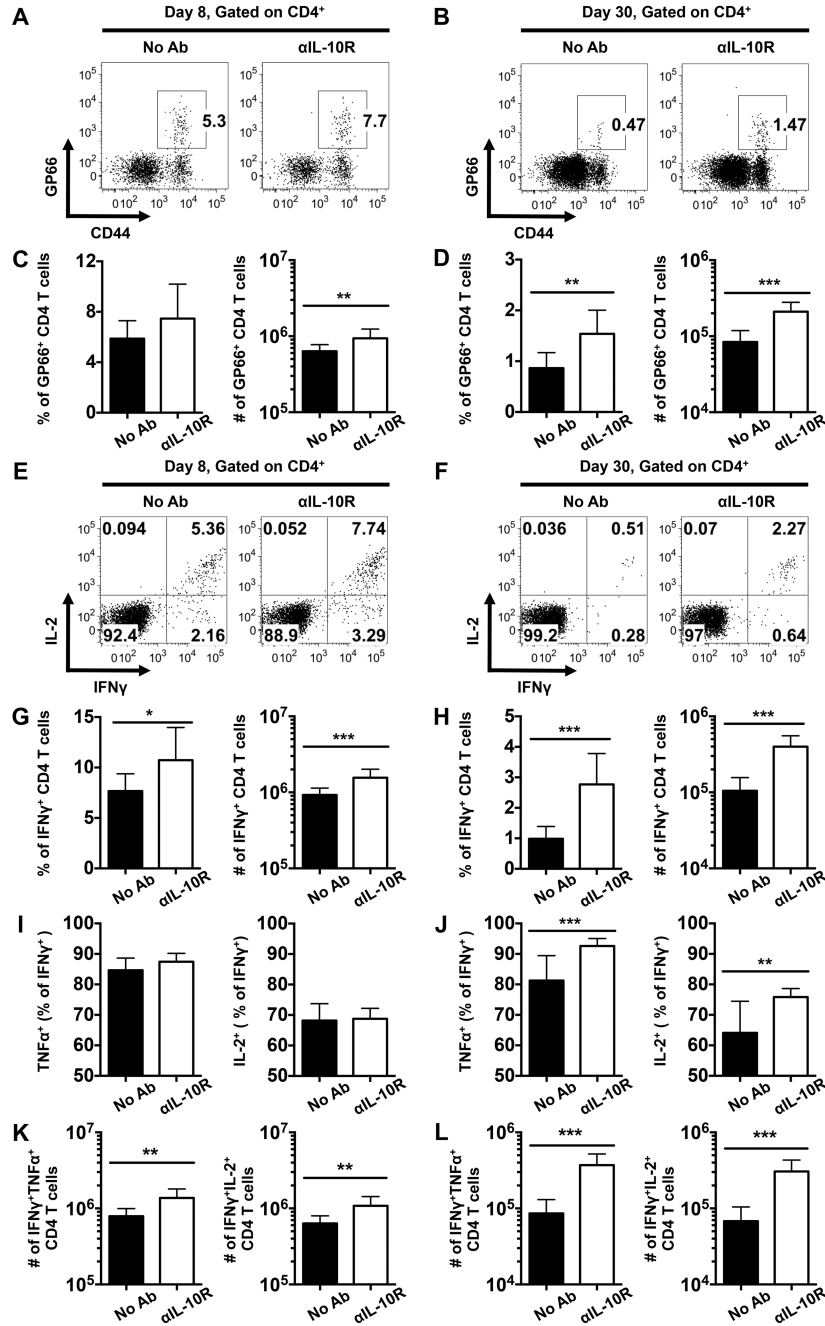


**FIGURE 4.** IL-10 signaling during the priming phase of infection suppresses effector and memory CD4 T cells. WT mice were infected with LCMV and either left untreated or treated with  $\alpha$ IL-10R antibodies at days 0, 2, 4, and 6 following infection. CD4 T cells in the spleens of infected mice were analyzed by flow cytometry at 8 and 30 days following infection. (A-B) Representative flow cytometry plots show the percentages of I-A<sup>b</sup> restricted GP66-specific CD4 T cells at (A) 8 or (B) 30 days following infection. (C-D) Bar graphs show the percentages (left panel) or numbers (right panel) of GP66-specific CD4 T cells at (C) day 8

or **(D)** day 30 following infection. **(E-L)** The production of IFN $\gamma$ , TNF $\alpha$ , and IL-2 by LCMV-specific CD4 T cells was analyzed by intracellular staining following stimulation with the GP61-80 peptide. **(E-F)** Representative dot plots show the expression of IL-2 and IFN $\gamma$  on gated CD4 T cells at **(E)** day 8 or **(F)** day 30 following infection. **(G-H)** Bar graphs show the percentages (left panel) or numbers (right panel) of IFN $\gamma$ -producing CD4 T cells at **(G)** day 8 or **(H)** day 30 following infection. **(I-L)** Bar graphs show the **(I, J)** proportion and **(K, L)** numbers of IFN $\gamma^+$  CD4 T cells that co-produce TNF $\alpha$  (left panels) or IL-2 (right panels) CD4 T cells at **(I, K)** 8 or **(J, L)** 30 days following infection. Representative or composite data are shown from two independent experiments analyzing 9–10 mice per group. \* $p < 0.05$ , \*\* $p < 0.01$ , \*\*\* $p < 0.001$ . Error bars show SD.

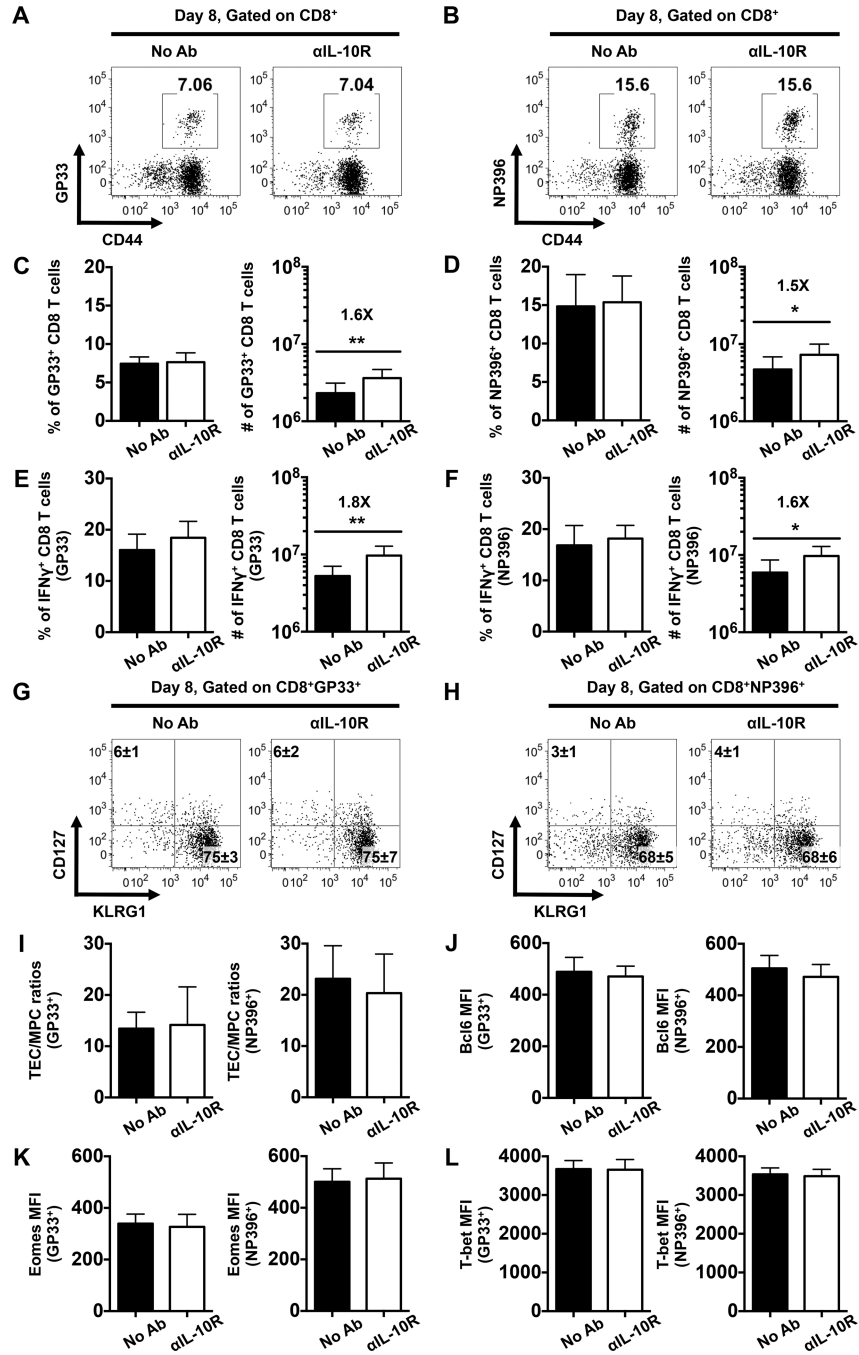


**FIGURE 5.**

IL-10 signaling during the priming phase of infection does not control the differentiation of effector CD8 T cells. WT mice were either left untreated or treated with αIL-10R antibodies at days 0, 2, 4, and 6 following LCMV infection, splenic CD8 T cells were then analyzed at day 8 following infection. (A-B) Representative dot plots show the percentages of LCMV (A) GP33-specific or (B) NP396-specific tetramer binding CD8 T cells. (C-D) Bar graphs show the percentages (left panel) or numbers (right panel) of (C) GP33- or (D) NP396-specific CD8 T cells. (E-F) Bar graphs show the percentages (left panel) or numbers (right

panel) of IFN $\gamma$ -producing CD8 T cells assessed by intracellular staining following stimulation with the (E) GP33-41 or (F) NP396-404 peptides. (G-H) Representative dot plots show the expression of CD127 and KLRG1 on gated (G) GP33- or (H) NP396-specific CD8 T cells. Numbers indicate the percentages  $\pm$  SD of MPCs (CD127<sup>high</sup>KLRG1<sup>low</sup>) and TECs (CD127<sup>low</sup>KLRG1<sup>high</sup>) tetramer-binding CD8 T cells. (I) Bar graphs show the ratios of GP33- (left panel) or NP396-specific (right panel) TECs to MPCs. (J-L) Bar graphs show the MFI of (J) Bcl6, (K) Eomes, and (L) T-bet levels in GP33- (left panel) or NP396-specific (right panel) CD8 T cells. Representative or composite data are shown from two independent experiments analyzing 9–10 mice per group. \* $p < 0.05$ , \*\* $p < 0.01$ . Error bars show SD.

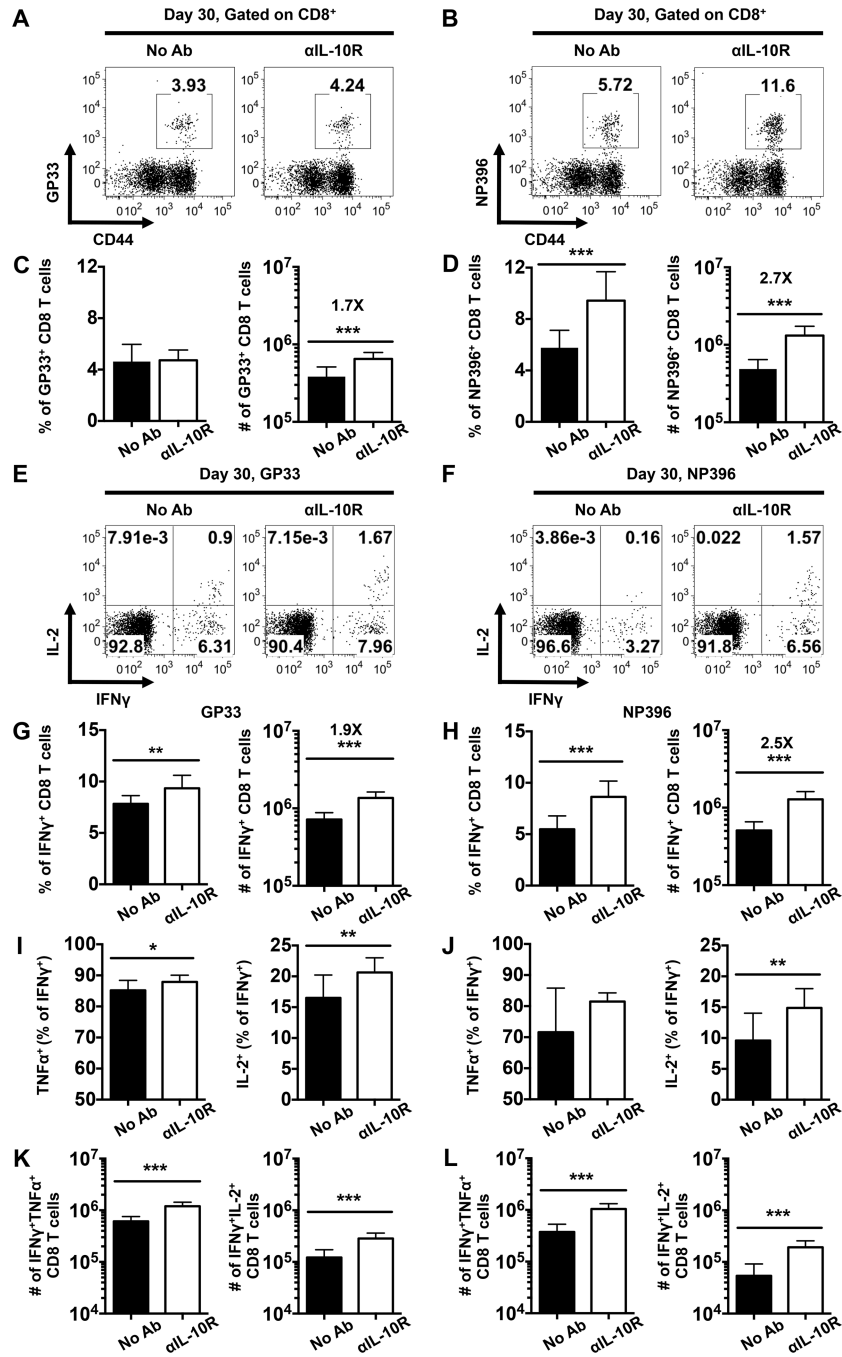


**FIGURE 6.** IL-10 signaling during the priming phase of infection negatively regulates the development of memory CD8 T cells. WT mice were either left untreated or treated with  $\alpha$ IL-10R antibodies at days 0, 2, 4, and 6 following LCMV infection. Splenic CD8 T cells were then analyzed at day 30 following infection. (A-B) Representative dot plots show the percentages of LCMV (A) GP33-specific or (B) NP396-specific tetramer binding CD8 T cells. (C-D) Bar graphs show the percentages (left panel) or numbers (right panel) of (C) GP33- or (D) NP396-specific CD8 T cells. (E-L) The production of IFN $\gamma$ , TNF $\alpha$ , and IL-2 by LCMV-

specific CD8 T cells was analyzed by intracellular staining following stimulation with GP33-44 or NP396-404 peptides. **(E-F)** Representative dot plots show the production of IL-2 and IFN $\gamma$  by **(E)** GP33- or **(F)** NP396-specific CD8 T cells. **(G-H)** Bar graphs show the overall percentages (left panel) or numbers (right panel) of **(G)** GP33- or **(H)** NP396-specific IFN $\gamma$ -producing CD8 T cells. **(I-J)** Bar graphs show the **(I, J)** proportion and **(K, L)** numbers of **(I, K)** GP33- or **(J, L)** NP396-specific CD8 T cells which co-produce IFN $\gamma$  and TNF $\alpha$  (left panels) or IFN $\gamma$  and IL-2 (right panels). Representative or composite data are shown from two independent experiments analyzing 9–10 mice per group. \* $p < 0.05$ , \*\* $p < 0.01$ , \*\*\* $p < 0.001$ . Error bars show SD.

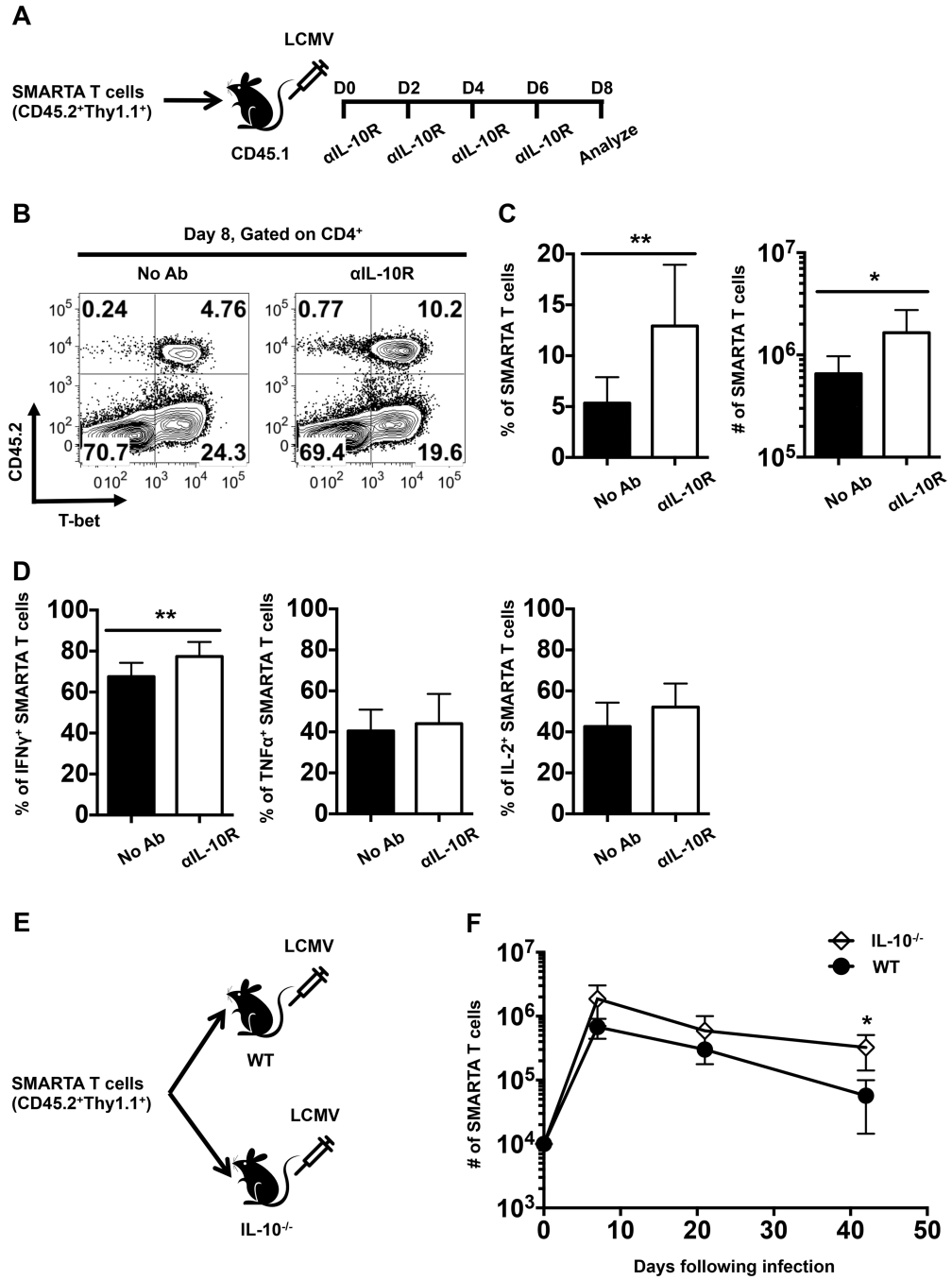


**FIGURE 7.** IL-10 regulates the magnitude of virus-specific CD4 T cell responses in an extrinsic manner. (A) Naïve SMARTA T cells were adoptively transferred into naïve CD45.1 recipient mice which were then subsequently infected with LCMV and either left untreated or treated with  $\alpha$ IL-10R antibodies at days 0, 2, 4, and 6 following infection. Splenic CD4 T cells were analyzed by flow cytometry at day 8 following infection. (B) Representative contour plots show the expression of CD45.2 and T-bet on gated splenic CD4 T cells at 8 days following infection. (C) Bar graphs show the percentages and numbers of donor CD45.2<sup>+</sup> SMARTA T

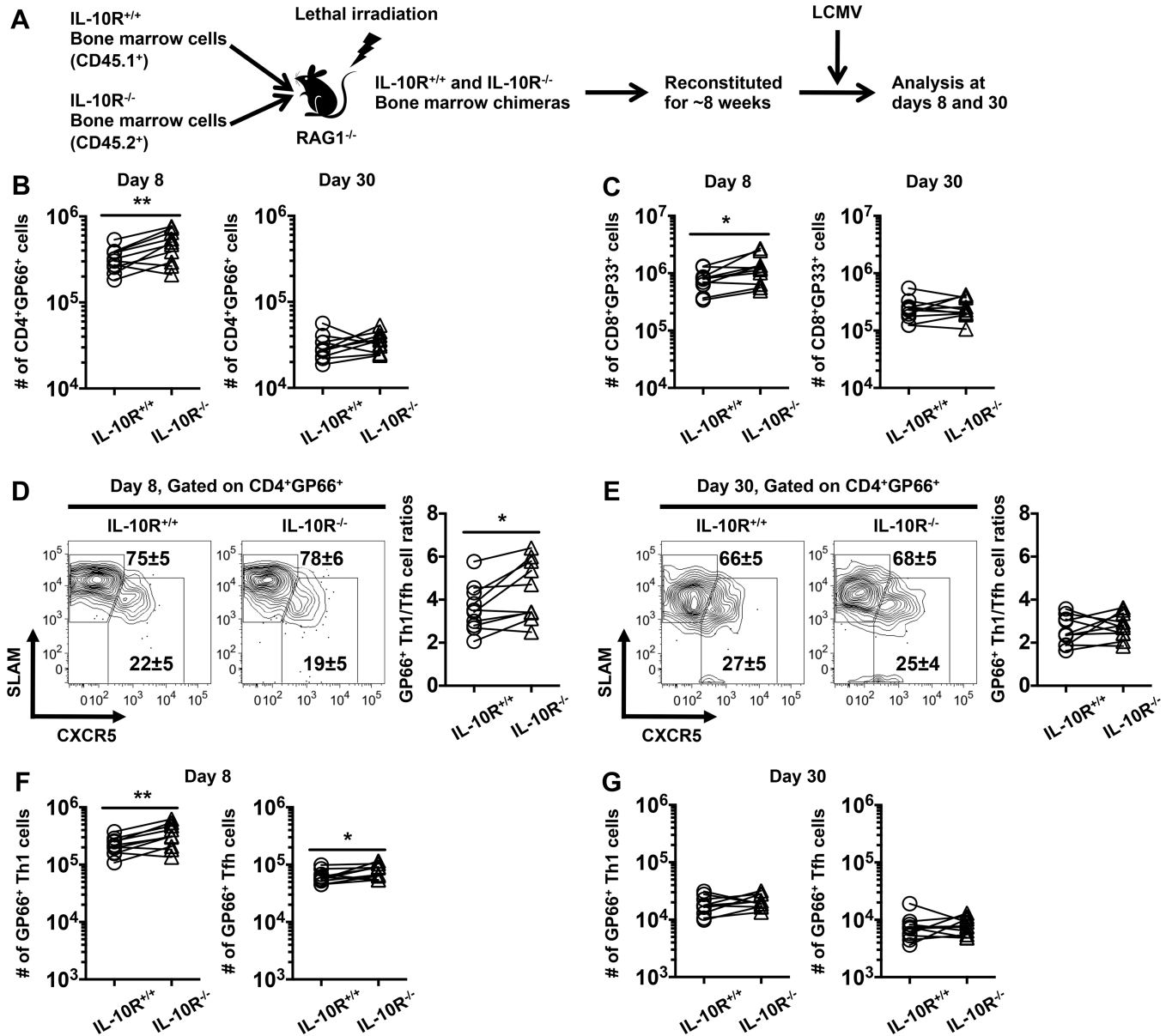
cells. **(D)** Graphs show the percentages of cytokine-producing donor SMARTA T cells assessed by intracellular staining following stimulation with the GP61-80 peptide. Representative or composite data are shown from two independent experiments analyzing 9 mice per group. **(E)** Schematic depicting the adoptive transfer of naïve SMARTA T cells into naïve WT or IL-10<sup>-/-</sup> mice which were subsequently infected with LCMV. **(F)** The numbers of donor SMARTA T cells in the spleens were evaluated at days 7, 21 and 42 following infection. Composite data are shown from two independent experiments analyzing 2–4 mice per group. \* $p < 0.05$ , \*\* $p < 0.01$ . Error bars show SD.

Author Manuscript

Author Manuscript

Author Manuscript

Author Manuscript

**FIGURE 8.**

Direct IL-10 signaling to T cells play minimal roles in the differentiation of anti-viral CD4 and CD8 T cells. (A) Schematic depicting the generation of IL-10R<sup>+/+</sup> and IL-10R<sup>-/-</sup> mixed bone marrow chimeras and the analytical strategy. (B, C) Graphs show the numbers of IL-10R<sup>+/+</sup> and IL-10R<sup>-/-</sup> (B) GP66-specific CD4 T cells or (C) GP33-specific CD8 T cells at day 8 (left panel) or day 30 (right panel) following infection. (D, E) Representative contour plots show the expression of SLAM and CXCR5 on gated IL-10R<sup>+/+</sup> and IL-10R<sup>-/-</sup> GP66<sup>+</sup> CD4 T cells at (D) 8 or (E) 30 days following infection. Numbers show the percentages  $\pm$  SD of Th1 (CXCR5<sup>low</sup>SLAM<sup>high</sup>, upper values) and Tfh (CXCR5<sup>high</sup>SLAM<sup>low</sup>, lower values) cells. Graphs show the ratios of GP66<sup>+</sup>Th1 to Tfh cells. (F, G) Graphs show the numbers of GP66-specific Th1 (left panel) or Tfh (right panel) cells at (F) 8 or (G) 30 days following infection. Representative or composite data are shown

from two independent experiments analyzing 10 mice per group. Each pair connected by line represents IL-10R<sup>+/+</sup> and IL-10R<sup>-/-</sup> T cell populations recovered from the same host. \* $p < 0.05$ , \*\* $p < 0.01$ .

Author Manuscript

Author Manuscript

Author Manuscript

Author Manuscript

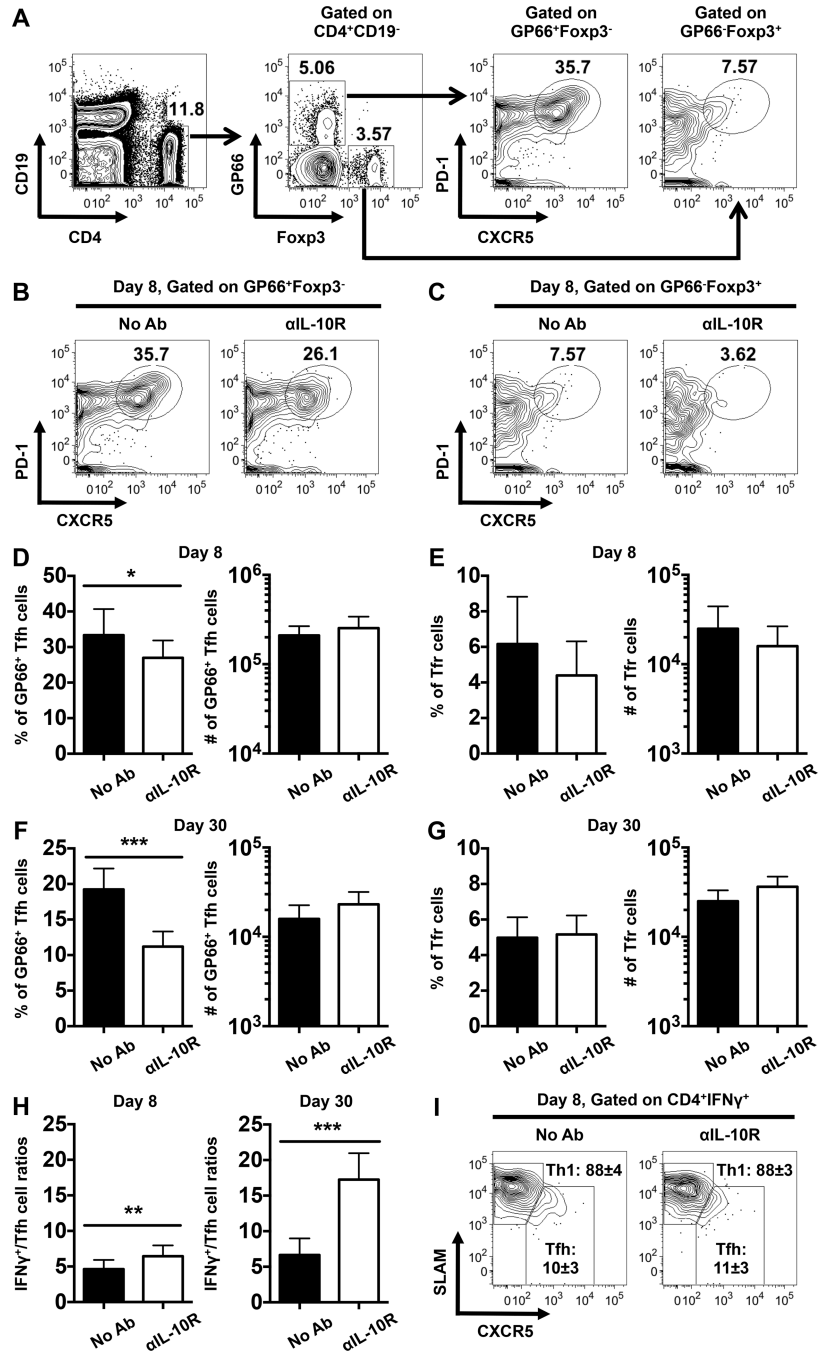


**FIGURE 9.**

The frequency but not number of LCMV-specific Tfh cells is reduced by IL-10R blockade signaling. WT mice were infected with LCMV and either left untreated or treated with αIL-10R antibodies at days 0, 2, 4, and 6 following infection. Splenic CD4 T cells were analyzed by flow cytometry at 8 and 30 days following infection. (A) Gating strategy for the identification of GP66-specific Tfh cells (CD4<sup>+</sup>CD19<sup>-</sup>GP66<sup>+</sup>Foxp3<sup>-</sup>CXCR5<sup>high</sup>PD-1<sup>high</sup>) and Tfr cells (CD4<sup>+</sup>CD19<sup>-</sup>GP66<sup>-</sup>Foxp3<sup>+</sup>CXCR5<sup>high</sup>PD-1<sup>high</sup>) cells. (B-C) Representative contour plots show the expression of PD-1 and CXCR5 on gated (B) GP66<sup>+</sup>Foxp3<sup>-</sup> or (C)

GP66<sup>-</sup>Foxp3<sup>+</sup> CD4 T cells. Numbers show the percentages of I-A<sup>b</sup>-restricted GP66-specific tetramer-binding Tfh or non-tetramer binding Foxp3<sup>+</sup> Tfr cells. **(D-G)** Bar graphs show the percentages (left panel) and numbers (right panel) of **(D, F)** GP66-specific Tfh cells and **(E, G)** Tfr cells at **(D, E)** day 8 or **(F, G)** 30 post infection. **(H)** Bar graphs show the ratios of IFN $\gamma$ <sup>+</sup> cells to GP66<sup>+</sup> Tfh cells at day 8 (left panel) and day 30 (right panel) post infection. In **(A-H)**, representative or composite data are shown from two independent experiments analyzing 9–10 mice per group. **(I)** Representative contour plots show the expression of SLAM and CXCR5 on gated IFN $\gamma$ <sup>+</sup> LCMV-specific CD4 T cells assessed following stimulation with the GP61-80 peptide at day 8 post infection. Numbers indicate the percentages  $\pm$  SD of Th1 cells (CXCR5<sup>low</sup>SLAM<sup>high</sup>, upper values) and Tfh cells (CXCR5<sup>high</sup>SLAM<sup>low</sup>, lower values). In **(I)**, representative data are shown from three independent experiments analyzing 14–15 mice per group. \* $p < 0.05$ , \*\* $p < 0.01$ , \*\*\* $p < 0.001$ . Error bars show SD.

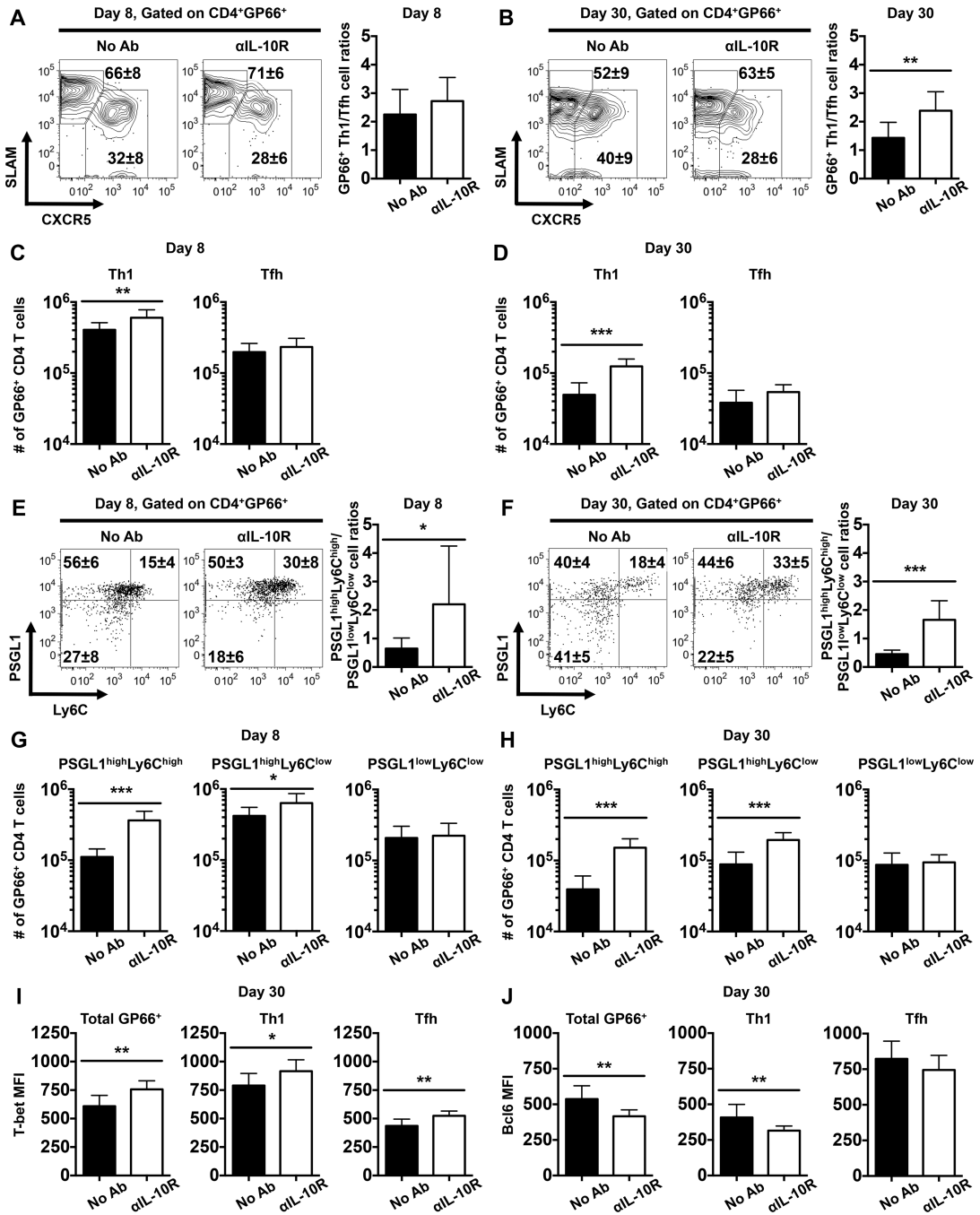


**FIGURE 10.**

IL-10 signaling during the priming phase of infection regulates the balance between antiviral Th1 and Tfh cells. WT mice were infected with LCMV and either left untreated or treated with αIL-10R antibodies at days 0, 2, 4, and 6 following infection. Splenic CD4 T cells were analyzed by flow cytometry at 8 and 30 days following infection. (A-B) Representative contour plots show the expression of SLAM and CXCR5 on gated GP66<sup>+</sup> CD4 T cells at (A) 8 or (B) 30 days following infection. Numbers show the percentages ± SD of CXCR5<sup>low</sup>SLAM<sup>high</sup> Th1 cells (upper values) and CXCR5<sup>high</sup>SLAM<sup>low</sup> Tfh cells

(lower values). Bar graphs show the ratios of GP66<sup>+</sup> Th1 to Tfh cells. **(C-D)** Bar graphs show the numbers of GP66-specific CXCR5<sup>low</sup>SLAM<sup>high</sup> Th1 (left panel) and CXCR5<sup>high</sup>SLAM<sup>low</sup> Tfh (right panel) cells at **(C)** 8 or **(D)** 30 days following infection. **(E-F)** Representative dot plots show the expression of PSGL1 and Ly6C on gated GP66<sup>+</sup> CD4 T cells at **(E)** 8 or **(F)** 30 days following infection. Numbers show the percentages  $\pm$  SD of cells in each quadrant. Bar graphs show the ratios of GP66<sup>+</sup> PSGL1<sup>high</sup>Ly6C<sup>high</sup> Th1 to PSGL1<sup>low</sup>Ly6C<sup>low</sup> Tfh cells. **(G-H)** Bar graphs show the numbers of GP66-specific PSGL1<sup>high</sup>Ly6C<sup>high</sup> (left panel), PSGL1<sup>high</sup>Ly6C<sup>low</sup> (middle panel), and PSGL1<sup>low</sup>Ly6C<sup>low</sup> (right panel) cells at **(G)** day 8 or **(H)** day 30 following infection. **(I-J)** Bar graphs show the MFI of **(I)** T-bet or **(J)** Bcl6 in total GP66<sup>+</sup> CD4 T cells (left panel), CXCR5<sup>low</sup>SLAM<sup>high</sup> Th1 cells (middle panel), and CXCR5<sup>high</sup>SLAM<sup>low</sup> Tfh cells (right panel) at day 30 post infection. Representative or composite data are shown from two independent experiments analyzing 9–10 mice per group. \* $p < 0.05$ , \*\* $p < 0.01$ , \*\*\* $p < 0.001$ . Error bars show SD.